Effect of tRNA maturase depletion on the levels and stabilities of ribosome assembly cofactor mRNAs in *Bacillus subtilis*

Aude Trinquier, Ciarán Condon* and Frédérique Braun*

*co-corresponding authors

CNRS, Université Paris Cité, Expression Génétique Microbienne,
Institut de Biologie Physico-Chimique, 13 rue Pierre et Marie Curie, 75005 Paris, France

Email: braun@ibpc.fr; condon@ibpc.fr

Key words: *RNA degradation, tRNA processing, translation, chloramphenicol, (p)ppGpp*

Abstract

The impact of translation on mRNA stability can be varied, ranging from a protective effect of ribosomes that shield mRNA from ribonucleases (RNases), to preferentially exposing sites of RNase cleavage. These effects can change depending on whether ribosomes are actively moving along the mRNA or whether they are stalled at particular sequences, structures or awaiting charged tRNAs. We recently observed that depleting *B. subtilis* cells of its tRNA maturation enzymes RNase P or RNase Z, led to altered mRNA levels of a number of assembly factors involved in the biogenesis of the 30S ribosomal subunit. Here, we extend this study to other assembly factor mRNAs and identify multiple transcriptional and translational layers of regulation of the *rimM* operon mRNA that occur in response to the depletion of functional tRNAs.

Importance

The passage of ribosomes across individual mRNAs during translation can have different effects on their degradation, ranging from a protective effect by shielding from ribonucleases, to in some cases, making the mRNA more vulnerable to RNase action. We recently showed that some mRNAs coding for proteins involved in ribosome assembly were highly sensitive to the availability of functional tRNA. Using strains depleted for the major tRNA processing enzymes RNase P and RNase Z, we expanded this observation to a wider set of mRNAs, including some unrelated to ribosome biogenesis. We characterize the impact of tRNA maturase depletion on the *rimM* operon mRNA and show it is highly complex, with multiple levels of transcriptional and post-transcriptional effects coming into play.

43 **Introduction**

44 The steady-state level of any mRNA in the cell is determined by both its rate of
45 transcription by RNA polymerase and its rate of degradation by ribonucleases (RNases).
46 These can work together to increase or decrease gene expression at the transcriptional or
47 post-transcriptional levels in response to environmental stimuli, or can pull in opposing
48 directions, resulting in little net gain. While most of the enzymes responsible for RNA decay
49 are now known in *B. subtilis* (1), how these enzymes are impacted by translation is still a
50 relatively open question. The conventional wisdom is that increased translation leads to
51 increased stability due to the masking of RNase cleavage sites by ribosomes. However, we
52 have recently identified an endoribonuclease (Rae1) that actually depends on translation to
53 destabilize mRNAs (2, 3), and we will present data here suggesting that antibiotics that cause
54 ribosome pausing can both positively and negatively impact mRNA levels, depending on the
55 severity and time of the dose.

56 Efficient translation depends on an unlimited supply of functional charged transfer RNAs
57 (tRNAs). tRNAs are almost universally transcribed as precursors in all living organisms, with
58 both 5' and 3' extensions that must be removed to generate tRNAs that can be charged and
59 used in translation. In *B. subtilis*, tRNAs are matured at their 5' end by the ubiquitous
60 endoribonuclease RNase P, consisting of a catalytic RNA moiety encoded by the *rnpB* gene
61 and a protein subunit encoded by the *rnpA* gene (4). Their 3' ends are matured either by the
62 endo/exoribonuclease RNase Z, or by a number of redundant 3' exoribonucleases,
63 depending nominally on whether the tRNA gene encodes the CCA motif required for
64 aminoacylation (5). RNase Z processes the one-third of *B. subtilis* tRNAs lacking an encoded
65 CCA-motif through stimulation of its endoribonuclease activity about 200-fold by a uracil
66 residue that naturally occurs ≤ 2 nts downstream of the so-called discriminator nucleotide
67 (nt 75) of each of these tRNA precursors (6). The enzyme's 3'-exoribonuclease activity is
68 required to trim back to nt 75 to allow addition of the CCA motif by nucleotidyl-transferase
69 (NTase or CCAse). Both RNase P and Z are essential in *B. subtilis* and depletion of either
70 enzyme inhibits cell growth, presumably due to a lack of functional tRNAs for translation.

71 Translation can also be inhibited by antibiotics that target the ribosome, such as
72 chloramphenicol (Cm), that that targets the peptidyl transferase center *(*PTC*)* located on the
73 large ribosomal subunit. Although it was once thought that Cm blocked translation
74 randomly, recent ribosome profiling experiments have shown that Cm preferentially causes

75 ribosomes to stall at particular sites, in particular when alanine (Ala) or serine (Ser) residues
76 have just been incorporated into the nascent peptide (7).

77 We have recently shown that depletion of tRNA maturase activity affects ribosome
78 assembly leading to a specific 30S subunit late assembly defect (8). While this defect was
79 mostly explained by a RelA-dependent accumulation of the stringent response alarmone
80 (p)ppGpp, and inhibition of GTP-dependent assembly factor activity, we also observed that
81 the levels of several mRNAs encoding ribosome assembly cofactors were affected. Notably,
82 the steady state levels of transcripts encoding the GTPases Era and YqeH were up-regulated
83 during tRNA maturase depletion, whereas mRNAs encoding the GTPase CpgA and the RNA
84 chaperone RimM were down-regulated. Because RNase P is thought to have very few direct
85 mRNA targets, and because RNase Z depletion had comparable effects on the expression of
86 these mRNAs, we considered it unlikely that the effects observed were directly due to RNase
87 P or RNase Z cleavages in each of these mRNAs. We therefore wished to better understand
88 by which mechanism(s) tRNA maturase depletion affected the levels of the cofactor
89 encoding mRNAs. Since the late 30S ribosome assembly defect observed in tRNA maturase
90 depletion strains was very similar to that observed in both *E. coli* and *B. subtilis ⊿rimM*
91 mutants, we put additional focus on exploring the decrease in *rimM* expression under these
92 conditions.

93 **Results**

94 **tRNA maturase depletion alters assembly factor mRNA levels**

95 We previously showed that depletion of RNase P or RNase Z results in altered mRNA
96 levels of four key 30S assembly cofactors (Era, YqeH, RimM and CpgA) (8). The effects of
97 depleting the RNA subunit of RNase P (RnpB) were more severe than the protein subunit
98 (RnpA), presumably because the RNA component of RNase P is more rapidly depleted than
99 the protein subunit once transcription is shut off. To ask whether this applied to other
100 mRNAs involved in ribosome biogenesis, we extended this analysis to the expression of
101 several other cofactor and ribosomal protein mRNAs, using xylose (*Pxyl-rnpA*) or IPTG-
102 dependent (*Pspac-rnpB* and *Pspac-rnz*) promoter constructs to deplete the protein and RNA
103 subunits of RNase P, and RNase Z, respectively. The two control transcripts, *yqeH* and *era,*
104 and three new transcripts, *ydaF* and *yjcK* (encoding two potential homologs of the *E. coli*

105 RimJ acetylase), and *rpsU* (encoding r-protein S21) were globally increased under conditions
106 of tRNA maturase depletion (Figure 1A), while *rimM*, *cpgA* (controls) and *yfmL* transcripts
107 (encoding a DEAD-box helicase), all showed decreased expression, with a visible
108 accumulation of degradation intermediates for *yfmL* (Figure 1B). Expression of the *rbfA* and
109 *ylxS/rimP* mRNAs were relatively unchanged (Figure 1C), showing that tRNA maturase
110 depletion does not cause non-specific perturbation of the expression of all *B. subtilis*
111 ribosome assembly cofactor genes. Although the primary focus of this study was on
112 assembly factor mRNAs because of the link to a defect in 30S biogenesis, we also asked
113 whether effects of tRNA maturase depletion could be seen on other mRNAs. Indeed, mRNAs
114 from the *yrzI* and *bmrCD* operons, encoding multiple peptides of unknown function and a
115 multi-drug resistance pump, respectively, were also up-regulated upon RNase P or RNase Z
116 depletion (Figure 1D), suggesting this phenomenon is not confined to mRNAs with ribosome-
117 related functions.
118

119 **tRNA maturase depletion and the translation inhibitor chloramphenicol alter mRNA**
120 **stability in a similar manner**

121 To determine whether tRNA maturase depletion impacted mRNA expression at the
122 transcriptional or post-transcriptional level, we measured the stability of several of these
123 mRNAs after rifampicin treatment in RNase P (RnpA or RnpB) depleted cultures. The up-
124 regulated transcripts (*yqeH, era, ydaF* and *yjcK*) were all stabilized during RnpA and RnpB
125 depletion (Figure 2A and B; Figure S1), suggesting that they are affected by RNase P
126 depletion at the post-transcriptional level. There is evidence that the lack of functional
127 tRNAs can increase ribosome stalling on translated mRNAs (9). Thus, the increased stability
128 of these transcripts could be due to ribosome stalling and the blocking of ribonuclease
129 access to cleavage sites on these mRNAs. To test this hypothesis, we sought to recapitulate
130 the effect by pausing translation in a different manner, using the translation elongation
131 inhibitor Cm. Indeed, the addition of sub-inhibitory (2.5 μg/mL) and minimal inhibitory (MIC;
132 5 μg/mL) concentrations of Cm to WT cells also increased the levels of the *yqeH, era, ydaF*
133 and *yjcK* mRNAs (Figure 2C), suggesting that the stabilization of these transcripts in tRNA
134 maturase depletion strains is most likely due to the lack of mature tRNA and ribosome
135 stalling.

136 The situation with the down-regulated transcripts was more complicated. The major
137 *rimM* (5, 3.5 and 1.8 kb) and *cpgA* (5 and 4.5 kb) transcripts were strongly destabilized in
138 RNase P RNA subunit (RnpB) depleted cells (Figure 3B; Figure S2), suggesting that the
139 decrease in expression also occurs at a post-transcriptional level in this strain. A similar
140 decrease in expression was seen after 30 minutes at high (MIC) Cm concentration in WT cells
141 for *rimM* and rapidly upon exposure to Cm for *cpgA* (Figure 3C), suggesting that this
142 phenomenon is also linked to ribosome stalling. For both *cpgA* and *yfmL*, the major
143 transcripts were processed to shorter forms in the absence of RnpB or in the presence of Cm
144 (Fig. 3B). One possibility is that, in contrast to the up-regulated mRNAs, when non-functional
145 tRNA precursors accumulate to high levels in the *rnpB*-depletion strain, ribosomes
146 eventually stall at sites that preferentially allow RNase access, or that the RNAs are largely
147 unoccupied by ribosomes.
148 In the less severely depleted *rnpA* strain, the full-length (5 kb) *rimM* transcript and the
149 two major *cpgA* mRNAs were stabilized (or showed little effect), rather than destabilized as
150 seen for *rnpB* (Figure 3A). These results suggest that down-regulation of *rimM* and *cpgA*
151 arises from a mixture of transcriptional (down) and post-transcriptional (up initially, then
152 down) effects and that one or other effect predominates depending on the severity of RNase
153 P depletion. Indeed, upon close inspection of Figure 3C, *rimM* and *cpgA* mRNA levels initially
154 increase at 15 mins and then decrease after further exposure to Cm at both sub-inhibitory
155 and MIC doses. Thus, the Cm effect globally tracks the effect of tRNA depletion, with the
156 weak Cm dose (2.5 μg/mL) mimicking the weak effect of depleting RnpA, and the strong Cm
157 dose (5 μg/mL) mimicking the strong effect of depleting RnpB, consistent with the notion of
158 opposing responses to severe *vs* less severe levels or duration of translation inhibition.

159 **Identification of *rimM*-containing transcripts sensitive to RNase P depletion**

160 Because the *ΔrimM* phenotype closely fitted the 30S late assembly defect observed in
161 strains depleted for RNase P or RNase Z (8), we attempted to narrow down the determinants
162 of the down-regulation of this operon. The *rimM* gene is encoded in a large operon
163 containing several genes encoding components of the translation machinery: ribosomal
164 protein genes *rpsP* and *rplS* (encoding S16 and L19, respectively), signal recognition particle
165 components (encoded by *ffh* and *ylxM*) and *trmD* that encodes a tRNA methyltransferase. To
166 identify the gene composition of the three *rimM*-containing transcripts, we performed

167 northern blots with probes located in ORFs of the neighboring genes (Figure S3). In all, six
168 different transcripts originate from this locus (Figure 4A). Promoters upstream of *ylxM* (P_1)
169 and *rplS* (P_3), and terminators downstream of *ylqC* and *rplS* (T_1 and T_3, respectively) were
170 identified earlier by transcriptome analysis (10). Our Northern blot analysis suggested that
171 two transcripts originate from P_1: the full-length mRNA (5 kb, highlighted in purple) that
172 terminates at T_3, and a shorter transcript (2.5 kb, highlighted in orange) that terminates at T_1
173 and does not contain the *rimM* ORF. The smallest species identified (0.5 kb, highlighted in
174 yellow) corresponds to the mono-cistronic *rplS* transcript (P_3 to T_3). Using end-enrichment
175 RNA sequencing (Rend-seq), DeLoughery *et al.* identified a third transcription start site (P_2)
176 located just upstream of *rpsP* and only 18 nts downstream of an RNase Y cleavage site in the
177 *ffh-rpsP* intergenic region, in addition to a potential terminator/attenuator (T_2) within the
178 *trmD* ORF (11). The three remaining transcripts (0.7 kb, highlighted in green; 1.8 kb, in cyan;
179 3 kb, in pink, and marked with an asterisk in Figure 4A) therefore correspond either to P_2
180 primary transcripts, or RNase Y-processed transcripts originating from P_1, which terminate at
181 T_1, T_2 and T_3, respectively. Interestingly, of the six transcripts encoded by this locus, only the
182 three containing both the *ylqD* and *rimM* ORFs were down-regulated upon RNase P
183 depletion (Figure 4B).

184 **A determinant for down-regulation of the *rimM* operon is located within the *ylqD* ORF**

185 To further narrow down which ORF was responsible for down-regulation of *rimM* operon
186 expression, we sub-cloned the *ylqD-rimM* or *rimM*-only parts of the operon under control of
187 a *Pspac* promoter, rendered constitutive by deleting the *lac* operator (Pspac(con); Table S3),
188 with an artificial terminator hairpin to provide a defined 3' end. The constructs were
189 integrated into the chromosome at the *amyE* locus and levels of the ectopic transcript were
190 analyzed by Northern blot in RNase P-depleted cells using a probe specific for *rimM*. The
191 steady state levels of the synthetic *ylqD-rimM* transcript were down-regulated in response
192 to RNase P depletion, albeit not as dramatically as the native operon (1.3- vs 2.3-fold),
193 suggesting that a determinant involved in down-regulation is still included in this shorter
194 construct (Figure 5A and B). Two degradation intermediates (~0.5 and ~0.4 kb in size) of the
195 *ylqD-rimM* transcript also accumulated, suggesting that this transcript is cleaved twice under
196 conditions of RnpB-depletion. It is possible that the weaker effect of RnpB-depletion the full-
197 length transcript and the accumulation of visible degradation intermediates is explained by

198 the presence of a stabilizing terminator hairpin at the 3' end of each of these species that is
199 not present in the native mRNA. Intriguingly, the construct containing only the *rimM* ORF
200 (with the same 3' terminator) was up-regulated in response to RNase P depletion (Figure 5C
201 and D). In combination, these results suggest that the region responsible for post-
202 transcriptional down-regulation of *rimM*-containing transcripts upon depletion of RNase P is
203 primarily located within the *ylqD* ORF.

204 Since unprocessed tRNAs accumulate in RNase P and RNase Z depleted cells, we
205 wondered whether they could act as potential post-transcriptional regulators of target
206 mRNAs by base pairing to their targets *via* their single stranded 5' and 3' extensions. Using
207 TargetRNA2 (12), a prediction program used for identifying targets of small RNAs (sRNAs) in
208 bacteria, we identified an 11-nt region within the *ylqD* ORF that could potentially base-pair
209 with the 5' immature extension of unprocessed *trnD-Tyr* tRNA (Figure 5B). To test whether
210 this sequence was involved in down-regulation of the *ylqD-rimM* construct in cells depleted
211 for RNase P, we weakened the putative base pairing interaction by introducing mutations in
212 the *ylqD* mRNA sequence (while maintaining the YlqD amino acid sequence as much as
213 possible) (Figure 5B). The mutant *ylqD*-rimM* construct was down-regulated and processed
214 similarly to the wt under conditions of RNase P depletion, suggesting that 5' extended *trnD-*
215 *Tyr* does not act as a post-transcriptional regulator of this operon. For the moment, the
216 sequence element(s) within *ylqD* responsible for down-regulation of the *rimM* operon under
217 conditions of tRNA maturase depletion remain(s) unknown.

218 **Down-regulation of *rimM* expression under physiological conditions resulting in reduced**
219 ***rnpA* expression is independent of immature tRNA accumulation**

220 We next asked whether the down-regulation of the *rimM operon* we observed during
221 RNase P depletion, would also occur in physiological conditions where RNase P expression is
222 reduced. The level of expression of the *rnpB* RNA is relatively constant in tiling array
223 experiments in over a hundred conditions tested, whereas *rnpA* mRNA levels decrease upon
224 ethanol addition and during stationary phase in both complex and minimal media (Figure
225 6A) (10). We confirmed that *rnpA* RNA expression was reduced to levels below detection in
226 these three conditions in comparison with exponential growth in the respective medium, by
227 Northern blot (Figure 6B). Ethanol treatment did not affect *rnpB* RNA levels; however, they
228 were reduced during stationary phase in both minimal and complex medium, in contrast to

229 the tiling array data. The expression of *rimM* varied similarly to *rnpA* in the conditions tested
230 (Figure 6B).

231 We next asked whether tRNA maturation was affected in stationary phase or upon
232 addition of ethanol using a probe for *trnJ-Lys* tRNA. Surprisingly, despite the decreased levels
233 of the *rnpA* mRNA in all three conditions, and *rnpB* in stationary phase, we did not observe
234 an accumulation of pre-tRNAs (Figure 6C). It is possible that very few new tRNA molecules
235 are synthesized under these conditions and/or that the remaining cellular RNase P activity
236 provided by the stable RnpA protein and RnpB RNA is sufficient to ensure the processing of
237 any that are transcribed. In either case, these experiments suggest that the down-regulation
238 of *rimM* expression that accompanies the decrease in *rnpA* and *rnpB* expression in stationary
239 phase or ethanol stress is more related to growth arrest than an accumulation of immature
240 tRNAs.

241 **Down-regulation of *rimM* in RNase P depletion strains depends partially on (p)ppGpp**
242 **production**

243 In bacteria, both stationary phase and ethanol stress are associated with increased
244 production of (p)ppGpp, hyperphosphorylated guanosine derivatives that are known to
245 globally reprogram transcription (13, 14). Considering that tRNA maturase-depleted cells
246 also trigger a RelA-dependent production of (p)ppGpp (8), we asked whether *rimM* down-
247 regulation in these cells was dependent on (p)ppGpp production, by measuring *rimM*
248 expression in (p)ppGpp^0 strains depleted for RnpA or RnpB. The (p)ppGpp^0 strain lacks the
249 three genes encoding (p)ppGpp synthesizing enzymes in *B. subtilis* (*yjbM, ywaC* and *relA*)
250 (15). If (p)ppGpp were the key mediator, we would expect that the effect of RNase P
251 depletion on *rimM* expression to be reduced or abolished in the (p)ppGpp^0 background.
252 Rather than simply abolishing the effect, *rimM* transcripts actually showed higher levels in
253 the tRNA maturase-depleted (p)ppGpp^0 strains compared to the RnpA or RnpB-depleted
254 strains capable of making (p)ppGpp (Figure 7A), suggesting that (p)ppGpp has an
255 independent repressive effect on *rimM* mRNA levels.

256 We thus assessed whether the alarmone (p)ppGpp could down-regulate *rimM*
257 expression in the absence of a tRNA processing defect using an engineered strain that allows
258 us to produce (p)ppGpp in the absence of immature tRNA accumulation or nutrient
259 starvation (8). This (p)ppGpp$^+$ strain consists of an ectopic copy of the *ywaC* gene placed

260 under the control of a *Pxyl* promoter in the (p)ppGpp^0 strain background. We used
261 derepression of the CodY-regulated *ywaA* mRNA as a proxy to follow the increase in
262 (p)ppGpp levels in this strain *in vivo* (Figure 7B) (8). We observed that (p)ppGpp induction
263 alone had no effect on the small (Y/P_2-T_2; cyan dot) *rimM* transcript, whereas the two larger
264 species (Y/P_2-T_3 and P_1-T_3, pink and purple dots, respectively) were down-regulated as the
265 expression of the (p)ppGpp reporter *ywaA* increased (Figure 7B). Although (p)ppGpp
266 production alone recapitulated what was seen in RnpB-depleted cells, the fact that only the
267 two larger transcripts behaved as expected from the results obtained in the RNase P-
268 depleted ppGpp^0 strain (Figure 7A), suggests that regulation of the smallest transcript (Y/P_2-
269 T_2) is more complex than simple transcriptional repression by (p)ppGpp.
270 The fact that the Y/P_2-T_2 *rimM* transcript could be down-regulated independently of
271 (p)ppGpp production led us to investigate the possibility of a further layer of regulation
272 where the growth slow-down in tRNA maturase-depleted cells would also affect *rimM*
273 expression by a mechanism independent of alarmone levels. To test this, we sought to
274 reproduce the growth rate defect by depleting for an unrelated essential enzyme. We
275 therefore performed Northern blot analysis on total RNA extracted from both RNase III (*rnc*)
276 depletion and deletion strains. The double-strand specific endoribonuclease RNase III is
277 essential in *B. subtilis* because it is required to silence expression of foreign toxin genes of
278 two prophages (Skin and SPβ) (16). Whereas depletion of RNase III in a WT background leads
279 to growth arrest, the *rnc* gene can be deleted in a strain lacking the two prophages without a
280 marked effect on growth rate. The RNase III depleted strain showed only a very limited
281 derepression of the CodY regulon in comparison with tRNA maturase-depleted strains
282 (Figure 8A) and did not accumulate visible amounts of (p)ppGpp on thin-layer
283 chromatography (TLC) (Figure 8B). This validates the use of RNase III depletion strains to
284 examine the effect of growth rate on *rimM* expression and to distinguish this from the effect
285 of accumulating high levels of (p)ppGpp. While RNase III deletion had no effect on *rimM*
286 expression, all three *rimM*-containing transcripts were strongly down-regulated during
287 RNase III depletion (Figure 8C), confirming that growth rate also plays a major role in the
288 regulation of *rimM* expression, independently of (p)ppGpp and tRNA maturase depletion.
289

290 **Discussion**

291 This study began with the observation that depletion of tRNA maturase enzymes in *B.*
292 *subtilis* led to a defect in 30S ribosome subunit assembly, which we showed was in part due
293 to an accumulation of (p)ppGpp and an inhibition of the activity of 30S assembly GTPases
294 (8). In our early attempts to understand the mechanism underlying this phenomenon, we
295 studied the expression of several 30S assembly factors and discovered that most were either
296 up or down-regulated at the mRNA level upon depletion of either RNase P or RNase Z.
297 We initially focused on the *rimM* mRNA because the 30S ribosome assembly defect
298 observed in tRNA maturase depletion mutants was very similar to that seen in a *ΔrimM*
299 strain. Although we later showed that ectopic *rimM* expression could not correct the
300 assembly defect in the *rnpB*-depleted strain (8), we were nonetheless curious about how
301 *rimM* expression was affected by the decrease in the levels of mature tRNAs. Together, our
302 data (summarized in Figure S4) indicate that the down-regulation of *rimM* transcript levels in
303 tRNA maturase-depleted cells is the result of a complex mixture of transcriptional and post-
304 transcriptional mechanisms, caused by a combination of effects mediated by a reduction in
305 growth rate, (p)ppGpp production and a translational defect due to lack of functional tRNAs,
306 with each layer of regulation capable of functioning independently of the others and
307 affecting the three *rimM* transcripts distinctly at different levels of severity.
308 We hypothesized that the accumulation of immature tRNAs during tRNA maturase
309 depletion increases ribosome stalling. Stalled ribosomes are known to affect mRNA decay in
310 bacteria (17) and a tRNA loss of function mutation leading to pre-tRNA processing defects
311 was reported to induce ribosome stalling in mice (9). In agreement with our hypothesis, we
312 observed that treatment with the translation elongation inhibitor chloramphenicol at MIC
313 concentrations recapitulates the effects of tRNA maturase depletion on the mRNA levels of
314 several different assembly factor mRNAs tested, four of which were up-regulated (*era, yqeH,*
315 *ydaF and yjcK)* and two down-regulated *(rimM* and *cpgA)*. Interestingly, Cm treatment at
316 sub-inhibitory concentrations did not impact cofactor mRNA levels in the same way, with
317 low Cm concentrations initially having transitory up-effects that were then reversed at
318 longer incubation times. One possibility is that short ribosome stalls transiently block access
319 to cleavage sites by housekeeping RNases such as RNase Y, resulting in mRNA stabilization,
320 while prolonged stalling could lead to mRNA destabilisation by an enzyme such as Rae1,
321 proposed to enter the A-site of stalled ribosomes (2), or by leaving large stretches of mRNA
322 unoccupied by ribosomes and vulnerable to cleavage by canonical degradation pathways.

323 Another notable difference between the two conditions is that the stringent response is
324 induced by Cm at MIC, as evidenced by the increase in expression the *ilvA* mRNA from the
325 CodY regulon (Figure S5), which could also contribute the increased severity of the response
326 to higher Cm concentrations. Activation of the stringent response in Cm-treated *B. subtilis*
327 was also previously observed by (18), consistent with our results. This is a marked difference
328 from *E. coli*, where Cm is a known inhibitor of stringent response induction (19, 20). The
329 mechanism still remains elusive in both cases.

330 Beyond their canonical role in protein synthesis, tRNAs have been implicated in the
331 regulation of several biological processes (for review, see (21, 22)). A new class of small non-
332 coding RNAs has emerged recently called tRNA-derived fragments (tRFs) or tRNA-derived
333 small RNAs, whose biological roles are not yet well understood (23). Different types of tRFs
334 differ in the cleavage position of the mature or precursor tRNA transcript. They have been
335 particularly studied in humans, where they have been shown to be involved in regulation of
336 a variety of cellular processes, including global translation, cellular proliferation, apoptosis
337 and epigenetic inheritance (24). Interestingly, a 3'-tRF in human cells plays an essential role
338 in fine-tuning ribosome biogenesis under normal physiological conditions by post-
339 transcriptionally regulating translation of at least two r-protein mRNAs (25). Although tRFs
340 have not yet been identified in *B. subtilis*, we asked whether pre-tRNAs could bind certain
341 assembly factor mRNAs *via* their 5' or 3' extensions and cause some of the post-
342 transcriptional effects observed in the tRNA maturase depletion strains. tRFs with 5' or 3'
343 extensions (pre-tRFs) could similarly behave as a new pool of potential regulatory sRNAs.
344 Although the potential base-pairing we identified between the 5' extension of trnD-Tyr and
345 the *rimM* transcripts does not seem to play a role in the down-regulation of *rimM*
346 expression, this doesn't preclude the possibility that other pre-tRNAs or pre-tRFs could be
347 involved in post-transcriptional regulatory events in *B. subtilis*.

348 A recent study in *E. coli* showed that the abundance of 46% of transcripts were affected
349 in a strain where the protein moiety of RNase P was heat denatured (26). The observation
350 that the addition of chloramphenicol mimicked the effect of tRNA maturase depletion in *B.*
351 *subtilis* for the upregulated mRNAs, and that down-regulation was the net result of a
352 mixture of translational and transcriptional effects, suggests that the effects seen on the *E.*
353 *coli* transcriptome may substantially be the result of ribosome stalling on mRNAs due to lack
354 of functional tRNAs, with differential impacts (up, down or neutral) on individual mRNA

stabilities or transcription levels. More detailed studies are required to untangle these effects on a global level in both organisms.

Acknowledgements

This work was supported by funds from the CNRS (UMR 8261), Université Paris Cité, the Agence Nationale de la Recherche (ARNr-QC). This work has been published under the framework of Equipex (Cacsice) and LABEX (Dynamo) programs that benefit from a state funding managed by the French National Research Agency as part of the Investments for the Future program. We thank lab members for helpful discussion.

364 **Materials and Methods**

365

366 **Strains and culture conditions**

367 All *B. subtilis* strains used were derived from our laboratory strain SSB1002, a W168
368 *trp*$^+$ prototrophic strain. Strains are listed in Table S1 and details of strains and plasmid
369 constructs are provided in Table S2 and S3, respectively. Oligonucleotides used are listed in
370 Table S4.

371 Unless stated otherwise, *B. subtilis* strains were grown in 2xYT liquid medium (1.6%
372 peptone, 1% yeast extract, 1% NaCl) at 200 rpm at 37°C in ≤ 1/10 volume of the flask to
373 ensure proper aeration. Overnight precultures were grown in presence of appropriate
374 antibiotics and inducer (1mM IPTG or 2% xylose), in the case of depletion strains.
375 Experimental cultures were grown in the absence of antibiotics, except where stated. For
376 depletion strains, overnight induced cultures were washed three times with pre-warmed
377 2xYT medium and inoculated at OD_{600} between 0.02 and 0.2, depending on the strain, in
378 fresh medium with or without inducer. Generally, induced cells were harvested for RNA
379 preparation around OD_{600} = 0.6 and cells grown in the absence of the inducer were followed
380 until they reach a plateau before being harvested. Inoculation and depletion conditions were
381 determined empirically for each strain such that the depleted cells were harvested between
382 OD_{600} = 0.3 and 0.7. For RnpA depletion, cultures were inoculated at OD_{600} = 0.05 in presence
383 of 2% xylose (inducer) or 2% glucose to tighten repression of the *Pxyl* promoter, which
384 typically led to a growth arrest (plateau) around OD_{600} = 0.6. For *rnz* and *rnpB* depletion
385 strains, cultures were inoculated in presence or in absence of 1mM IPTG at OD_{600} = 0.05 and
386 OD_{600} = 0.2, respectively. RNase Z and RnpB depleted cells typically plateau around OD_{600} =
387 0.6 and OD_{600}= 0.3, respectively.

388 For rifampicin experiments, *B. subtilis* strains were grown in 2xTY at 37°C with shaking as
389 described above. At OD_{600nm} = 0.6 (or less for some depletion strains), rifampicin was added
390 to a final concentration of 150 µg/mL in order to block new RNA synthesis. Samples were
391 collected at different time points (e. g. 0, 2, 5, 10, 15 and 20 minutes) by mixing the cells
392 with frozen 10 mM sodium azide (200 µL for 1.3 mL culture). Samples were vortexed until
393 the sodium azide thawed, cells were pelleted by centrifugation at 4°C and the pellet was
394 conserved at -20°C until RNA extraction.

395 To mimic amino acid starvation, we depleted charged arginine tRNAs by addition of
396 arginine hydroxamate (RHX) at 250 mg/mL in cultures growing in 2xTY at OD_{600} = 0.3.
397 To study the effect of translation pausing, we added the translation elongation inhibitor
398 chloramphenicol (Cm) at sub-inhibitory (2.5 µg/ml) or minimal inhibitory concentration (5
399 µg/ml) to cells growing in 2xYT at OD_{600} = 0.6. Cells were harvested just before Cm addition
400 (t_0) and 15, 30 and 60 mins after treatment.
401 To reproduce some growth conditions from the *B. subtilis* tiling array experiment (10) known
402 to lead to a decrease in *rnpA* expression, ethanol was added to cultures growing in minimal
403 medium (M9 with 0.5 % glucose) at 4% (v/v) around OD_{600} = 0.4 and cells were harvested 10
404 mins after treatment.
405
406 **Plasmid constructs**
407 The *rimM* gene was amplified by PCR using oligo pair (CC2034/CC1986) and cloned between
408 the BamHI and XhoI sites of the integrative pHM2-Pspac(con) vector (Table S3). The
409 bicistronic *ylqD-rimM* construct was amplified by PCR using oligo pair (CC1985/CC1986) and
410 cloned between the BamHI and SalI sites of pHM2-Pspac(con). The mutated construct *ylqD*-*
411 *rimM* was obtained by two-fragment overlapping PCR. The upstream fragment was
412 amplified with the forward primer CC1985 and the reverse primer CC2012 and the
413 downstream fragment with the forward primer CC2011 and the reverse primer CC1986. The
414 overlapping fragments were reamplified using oligo pair CC1985/CC1986 and cloned
415 between the BamHI and SalI sites of pHM2-Pspac(con). The integrative plasmids were
416 linearized with XbaI before transformation, for integration into the *amyE* locus of the *B.*
417 *subtilis* chromosome.
418
419 **RNA extraction and Northern blots**
420 RNA extraction was typically performed using the glass beads/phenol protocol
421 (adapted from (27)) on 1 to 8 mL mid-log phase *B. subtilis* cells growing in 2xYT.
422 To perform Northern blots, 5 µg total RNA were denatured for 5 mins at 95°C in RNA
423 Gel loading dye (Thermo Scientific) before being separated on 1% agarose gels in 1X TBE
424 (native) or on denaturing 5% acrylamide gels in 1X TBE + 7M urea. RNA was transferred from

425 agarose gels to a hybond-N membrane (GE-Healthcare) by capillary transfer for 4 hours
426 minimum in 1X transfer buffer (5X SSC, 0.01M NaOH). For Northerns of acrylamide gels, RNA
427 was electro-transferred at 4°C in 0.5X TBE for 4 hours at 60V or overnight at 12V. RNA was
428 cross-linked to the membrane by UV cross-linking at 120,000 microjoules/cm^2 using HL-200
429 Hybrilinker UV-crosslinker (UVP). Probes for Northern blots were usually 25 to 30-nt DNA
430 oligonucleotides radiolabeled on their 5' end by polynucleotide kinase. The *cpgA* mRNA was
431 detected using a riboprobe using a PCR fragment amplified using oligos CC2200 and CC2201
432 as template. Membranes were pre-incubated in Ultra-Hyb (Life Technologies) for agarose
433 blots or Roti-Hybri-Quick (Roth) for acrylamide blots for 1 hour and hybridized with
434 radiolabeled probes for a minimum of 4 hours. Pre-incubation, hybridization and wash steps
435 were performed at 42°C in the case of 5'-labeled oligonucleotides or at 68°C for riboprobes.
436 Membranes were quickly rinsed once at room temperature in 2x SSC 0.1% SDS to remove
437 non-hybridized probe before being washed once for 5 mins in the same buffer and then
438 twice for 5 mins in 0.2x SSC 0.1% SDS. Northerns were exposed to PhosphorImager screens
439 (GE Healthcare) and the signal was obtained by scanning with a Typhoon scanner (GE
440 Healthcare) and analyzed by Fiji (ImageJ) software.
441
442 **Thin layer chromotagraphy (TLC)**
443 TLC analysis was used to detect radiolabeled (p)ppGpp as described in (8).
444
445

446 **References**

447 1. **Condon C, Bechhofer DH.** 2011. Regulated RNA stability in the Gram positives. Curr
448 Opin Microbiol 14:148-54.
449 2. **Leroy M, Piton J, Gilet L, Pellegrini O, Proux C, Coppee JY, Figaro S, Condon C.** 2017.
450 Rae1/YacP, a new endoribonuclease involved in ribosome-dependent mRNA decay in
451 Bacillus subtilis. EMBO J 36:1167-1181.
452 3. **Condon C, Piton J, Braun F.** 2018. Distribution of the ribosome associated
453 endonuclease Rae1 and the potential role of conserved amino acids in codon
454 recognition. RNA Biol doi:10.1080/15476286.2018.1454250:1-6.
455 4. **Braun F, Condon C**. 2019. RNA processing, p 164-177 *In* Schmidt TM (ed),
456 Encyclopedia of Microbiology, 4th edition doi:10.1016/B978-0-12-801238-3.02455-7.
457 Elsevier.
458 5. **Wen T, Oussenko IA, Pellegrini O, Bechhofer DH, Condon C.** 2005. Ribonuclease PH
459 plays a major role in the exonucleolytic maturation of CCA-containing tRNA
460 precursors in Bacillus subtilis. Nucleic Acids Res 33:3636-43.
461 6. **Pellegrini O, Li de la Sierra-Gallay I, Piton J, Gilet L, Condon C.** 2012. Activation of
462 tRNA maturation by downstream uracil residues in B. subtilis. Structure 20:1769-77.
463 7. **Marks J, Kannan K, Roncase EJ, Klepacki D, Kefi A, Orelle C, Vazquez-Laslop N,**
464 **Mankin AS.** 2016. Context-specific inhibition of translation by ribosomal antibiotics
465 targeting the peptidyl transferase center. Proc Natl Acad Sci U S A 113:12150-12155.
466 8. **Trinquier A, Ulmer JE, Gilet L, Figaro S, Hammann P, Kuhn L, Braun F, Condon C.**
467 2019. tRNA Maturation Defects Lead to Inhibition of rRNA Processing via Synthesis of
468 pppGpp. Mol Cell 74:1227-1238 e3.
469 9. **Ishimura R, Nagy G, Dotu I, Zhou H, Yang XL, Schimmel P, Senju S, Nishimura Y,**
470 **Chuang JH, Ackerman SL.** 2014. RNA function. Ribosome stalling induced by
471 mutation of a CNS-specific tRNA causes neurodegeneration. Science 345:455-9.
472 10. **Nicolas P, Mader U, Dervyn E, Rochat T, Leduc A, Pigeonneau N, Bidnenko E,**
473 **Marchadier E, Hoebeke M, Aymerich S, Becher D, Bisicchia P, Botella E, Delumeau**
474 **O, Doherty G, Denham EL, Fogg MJ, Fromion V, Goelzer A, Hansen A, Hartig E,**
475 **Harwood CR, Homuth G, Jarmer H, Jules M, Klipp E, Le Chat L, Lecointe F, Lewis P,**
476 **Liebermeister W, March A, Mars RA, Nannapaneni P, Noone D, Pohl S, Rinn B,**
477 **Rugheimer F, Sappa PK, Samson F, Schaffer M, Schwikowski B, Steil L, Stulke J,**
478 **Wiegert T, Devine KM, Wilkinson AJ, van Dijl JM, Hecker M, Volker U, Bessieres P,**
479 **et al.** 2012. Condition-dependent transcriptome reveals high-level regulatory
480 architecture in Bacillus subtilis. Science 335:1103-6.
481 11. **DeLoughery A, Lalanne JB, Losick R, Li GW.** 2018. Maturation of polycistronic mRNAs
482 by the endoribonuclease RNase Y and its associated Y-complex in Bacillus subtilis.
483 Proc Natl Acad Sci U S A 115:E5585-E5594.
484 12. **Kery MB, Feldman M, Livny J, Tjaden B.** 2014. TargetRNA2: identifying targets of
485 small regulatory RNAs in bacteria. Nucleic Acids Res 42:W124-9.
486 13. **Murray HD, Schneider DA, Gourse RL.** 2003. Control of rRNA expression by small
487 molecules is dynamic and nonredundant. Mol Cell 12:125-34.
488 14. **VanBogelen RA, Kelley PM, Neidhardt FC.** 1987. Differential induction of heat shock,
489 SOS, and oxidation stress regulons and accumulation of nucleotides in Escherichia
490 coli. J Bacteriol 169:26-32.

491 15. **Kriel A, Bittner AN, Kim SH, Liu K, Tehranchi AK, Zou WY, Rendon S, Chen R, Tu BP,**
492 **Wang JD.** 2012. Direct regulation of GTP homeostasis by (p)ppGpp: a critical
493 component of viability and stress resistance. Mol Cell 48:231-41.
494 16. **Durand S, Gilet L, Condon C.** 2012. The essential function of B. subtilis RNase III is to
495 silence foreign toxin genes. PLoS Genet 8:e1003181.
496 17. **Deana A, Belasco JG.** 2005. Lost in translation: the influence of ribosomes on
497 bacterial mRNA decay. Genes Dev 19:2526-33.
498 18. **Rhaese HJ, Dichtelmuller H, Grade R.** 1975. Studies on the control of development.
499 Accumulation of guanosine tetraphosphate and pentaphosphate in response to
500 inhibition of protein synthesis in Bacillus subtilis. Eur J Biochem 56:385-92.
501 19. **Cashel M.** 1969. The control of ribonucleic acid synthesis in Escherichia coli. IV.
502 Relevance of unusual phosphorylated compounds from amino acid-starved stringent
503 strains. J Biol Chem 244:3133-41.
504 20. **Kurland CG, Maaloe O.** 1962. Regulation of ribosomal and transfer RNA synthesis. J
505 Mol Biol 4:193-210.
506 21. **Katz A, Elgamal S, Rajkovic A, Ibba M.** 2016. Non-canonical roles of tRNAs and tRNA
507 mimics in bacterial cell biology. Mol Microbiol 101:545-58.
508 22. **Raina M, Ibba M.** 2014. tRNAs as regulators of biological processes. Front Genet
509 5:171.
510 23. **Lee YS, Shibata Y, Malhotra A, Dutta A.** 2009. A novel class of small RNAs: tRNA-
511 derived RNA fragments (tRFs). Genes Dev 23:2639-49.
512 24. **Kumar P, Kuscu C, Dutta A.** 2016. Biogenesis and Function of Transfer RNA-Related
513 Fragments (tRFs). Trends Biochem Sci 41:679-689.
514 25. **Kim HK, Fuchs G, Wang S, Wei W, Zhang Y, Park H, Roy-Chaudhuri B, Li P, Xu J, Chu**
515 **K, Zhang F, Chua MS, So S, Zhang QC, Sarnow P, Kay MA.** 2017. A transfer-RNA-
516 derived small RNA regulates ribosome biogenesis. Nature 552:57-62.
517 26. **Mohanty BK, Kushner SR.** 2022. Inactivation of RNase P in Escherichia coli
518 significantly changes post-transcriptional RNA metabolism. Mol Microbiol 117:121-
519 142.
520 27. **Bechhofer DH, Oussenko IA, Deikus G, Yao S, Mathy N, Condon C.** 2008. Analysis of
521 mRNA decay in Bacillus subtilis. Methods Enzymol 447:259-76.
522 28. **Wegscheid B, Condon C, Hartmann RK.** 2006. Type A and B RNase P RNAs are
523 interchangeable in vivo despite substantial biophysical differences. EMBO Rep 7:411-
524 7.
525 29. **Koo BM, Kritikos G, Farelli JD, Todor H, Tong K, Kimsey H, Wapinski I, Galardini M,**
526 **Cabal A, Peters JM, Hachmann AB, Rudner DZ, Allen KN, Typas A, Gross CA.** 2017.
527 Construction and Analysis of Two Genome-Scale Deletion Libraries for Bacillus
528 subtilis. Cell Syst 4:291-305 e7.
529 30. **Chary VK, Amaya EI, Piggot PJ.** 1997. Neomycin- and spectinomycin-resistance
530 replacement vectors for Bacillus subtilis. FEMS Microbiol Lett 153:135-9.
531 31. **Gendron N, Putzer H, Grunberg-Manago M.** 1994. Expression of both *Bacillus subtilis*
532 threonyl-tRNA synthetase genes is autogenously regulated. J Bacteriol 176:486-494.
533

534

535 **Figure Legends**

536 **Figure 1.** Depletion of tRNA processing enzymes results in perturbed expression of some
537 mRNAs encoding proteins involved in 30S subunit assembly. Northern blots showing (A) Up-
538 regulated mRNAs, (B) Down-regulated mRNAs (C) Unaffected mRNAs and (D) mRNAs
539 unrelated to ribosome assembly, present in total mRNA isolated in the presence or absence
540 of inducer as indicated. Note that the basal level of the *bmrCD* transcript, encoding a
541 multidrug transporter, is higher in the *Pspac-rnz* and *Pspac-rnpB* strains because of the
542 presence of erythromycin in the medium for stable maintenance of the construct. 16S rRNA
543 levels (ethidium bromide stained) are shown as a loading control. Series of blots where a
544 single loading control is shown, were stripped and reprobed. The blots for *era, yqeH, rimM*
545 and *cpgA* were regenerated as in ref. (8) with independent RNA preparations, with
546 permission granted by the publisher for re-use of previously published data. Number of
547 repetitions (n) as follows: *yqeH* (n=3); *era* (n=3); *rpsU* (n=4); *ydaF* (n=2); *yjcK* (n=2); *rimM*
548 (n=3); *cpgA* (n=3); *rbfA* (n=2); *ylxS* (n=2); *yfmL* (n=2); *bmrCD* (n=2); *yrzI* (n=2).

549

550 **Figure 2.** Up-regulated mRNAs show increased stability upon tRNA maturase depletion and
551 increased expression levels in the presence of chloramphenicol. Northern blots of total RNA
552 isolated at different times after addition of rifampicin (Rif) in cells grown in the presence or
553 absence of inducer for (A) *rnpB* or (B) *rnpA* expression. Transcript sizes are given in kb to the
554 left of the blots and half-lives are reported under each blot. Note, that since *yjcK* gives no
555 signal in the presence of inducer, we cannot rule out a transcriptional effect in this case. (C)
556 Northern blots of total RNA isolated at different times after addition of 0.5x MIC and MIC of
557 chloramphenicol (Cm). 16S rRNA levels (ethidium bromide stained) are shown as a loading
558 control. Series of blots where a single loading control is shown, were stripped and reprobed.
559 Experiments were performed twice, with decay plots and their quantifications given in
560 Figure S1.

561

562 **Figure 3.** Downregulated mRNAs are subjected to a mixture of transcriptional and post-
563 transcriptional effects upon tRNA maturase depletion and chloramphenicol addition.
564 Northern blots of total RNA isolated at different times after addition of rifampicin (Rif) in
565 cells grown in the presence or absence of inducer for (A) *rnpB* or (B) *rnpA* expression.

566 Transcript sizes are given in kb to the left of the blot and half-lives are reported under each
567 blot. (C) Northern blots of total RNA isolated at different times after addition of 0.5x MIC
568 and MIC of chloramphenicol (Cm). 16S rRNA levels (ethidium bromide stained) are shown as
569 a loading control. Series of blots where a single loading control is shown, were stripped and
570 reprobed. Blots shown in Fig. 2 were stripped and reprobed for use in this figure.
571 Experiments were performed twice, with decay plots and their quantifications given in
572 Figure S2.

573

574 **Figure 4.** Three of the six transcripts emanating from the *rimM* operon are sensitive to tRNA
575 maturase depletion. (A) Structure of the *rimM* operon. Open reading frames (ORFs; not to
576 scale) are shown as gray arrows and transcripts as different colored wavy lines. Sizes are as
577 indicated. Promoters (P_1-P_3) are represented by black arrows and terminators (T_1-T_3) as
578 hairpins. A known RNase Y cleavage site is indicated by a scissors symbol. The asterisk
579 indicates transcripts that may be processed by RNase Y, but are not distinguishable from P_2
580 primary transcripts by Northern blot. These are denoted Y/P2 in the text. (B) Northern blot
581 analysis of total RNA from *Pxyl-rnpA* cells grown in the presence or absence of inducer,
582 probed with oligonucleotides targeting different ORFs of the operon (indicated below
583 panel). Colored dots correspond to the colors of the transcripts shown in panel A.

584

585 **Figure 5.** A determinant for down regulation of the *rimM* operon in response to tRNA
586 maturase depletion is located within the *ylqD* ORF. (A) Northern blot of total RNA from
587 *Pspac-rnpB* cells isolated in the presence or absence of IPTG showing the effect of RnpB-
588 depletion on expression of an ectopic *ylqD-rimM* short operon containing a wt or mutated
589 (*) potential target sequence for *trnD-Tyr* pre-tRNA within the *ylqD* ORF. Colored dots
590 identifying endogenous *rimM* transcripts follow the same code as in Figure 4. (B) Schematic
591 of ectopic *ylqD-rimM* constructs placed under control of the constitutive promoter (P) used
592 in panel A. The zoom in shows the complementarity to the *trnD-Tyr* pre-tRNA and its
593 disruption in the *ylqD*-rimM* mutant construct. Coordinates are relative to the start codon
594 of *rimM*. (C) Northern blot showing the effect of RNase P depletion (*rnpA* or *rnpB*) on
595 expression of an ectopic *rimM*-only construct. (D) Schematic of ectopic *rimM* construct
596 placed under control of the constitutive promoter (P) used in panel C. Slower migrating

597 bands (marked with an asterisk) are likely due to read-through of the terminator in the
598 ectopic construct. 16S rRNA levels (ethidium bromide stained) are shown as a loading
599 control.
600
601 **Figure 6.** Ethanol stress and stationary phase affect *rnpA* and *rnpB* expression without
602 causing tRNA processing defects. (A) *rnpB* (black) and *rnpA* (red) transcript levels over 100
603 different growth conditions (from ref. (10)). The three conditions indicated in yellow
604 (ethanol stress and stationary phase in complex and minimal medium) result in reduced
605 *rnpA* RNA levels. For each condition, *rnpA* and *rnpB* RNA levels (log2) are indicated in the
606 yellow box. (B) Northern blot comparing *rnpB* (first panel, acrylamide gel because of small
607 size, 401 nts), *rnpA* and *rimM* (second and third panel, agarose gel) RNA levels, after ethanol
608 addition (EtOH) or during exponential (Exp) or stationary (Stat) phase in minimum (MM) or
609 complex (2xTY) medium. Colored dots identifying *rimM* transcripts follow the same code as
610 in Figure 4. Note that the 16S rRNA (loading control) is beginning to be degraded in MM
611 stationary phase. (C) Northern blot probed for *trnJ-Lys* (acrylamide gel) showing no pre-tRNA
612 accumulation in the different conditions tested. See Figure S1 of ref. (8) for accumulation of
613 *trnJ-Lys* precursors under conditions of RnpA and RnpB depletion.
614
615 **Figure 7.** Influence of (p)ppGpp on *rimM* expression. (A) Northern blot comparing the effect
616 of RNase P depletion (RnpB or RnpA) on *rimM* expression in a wt and (p)ppGpp^0 background.
617 (B) Northern blot of *rimM* expression after induction of (p)ppGpp production using a xylose
618 inducible *ywaC* in a *ΔyjbM ywaC relA* ((p)ppGpp^0) background. Colored dots identifying *rimM*
619 transcripts follow the same code as in Figure 4. 16S rRNA levels (ethidium bromide stained)
620 are shown as a loading control. Series of blots where a single loading control is shown, were
621 stripped and reprobed. Note that this Northern blot was generated by reprobing a
622 membrane previously used in ref. (8), with permission to re-use the *ywaA* control panel
623 granted by the publisher.
624
625 Figure 8. Expression of the *rimM* operon is regulated by growth rate independent of
626 (p)ppGpp. (A) Northern blot comparing the effect of RNase III deletion, and RNase P or
627 RNase III depletion on derepression of the CodY-regulated *ywaA mRNA.* (B) RNase III-

628 depleted cells do not accumulate large amounts of (p)ppGpp compared to tRNA maturase
629 depleted ones. Thin-layer chromatography (TLC) analysis of ^{32}P-labeled nucleotides
630 extracted from RNase III-depleted cells (*rnc*). Arginine hydroxamate (RHX; 250mg/mL) was
631 added to wt and (p)ppGpp^{0} strains as positive and negative controls. The top and bottom
632 halves are exposed for different times. Note that this is a re-crop of an image previously
633 published in ref. (8); the first four (control) lanes are reshown to show the migration position
634 of (p)ppGpp, with permission from the publisher. (C) Northern blot comparing the effect of
635 RNase III depletion or deletion on *rimM* expression. Colored dots identifying *rimM*
636 transcripts follow the same code as in Figure 4. 16S rRNA levels (ethidium bromide stained)
637 are shown as a loading control.
638

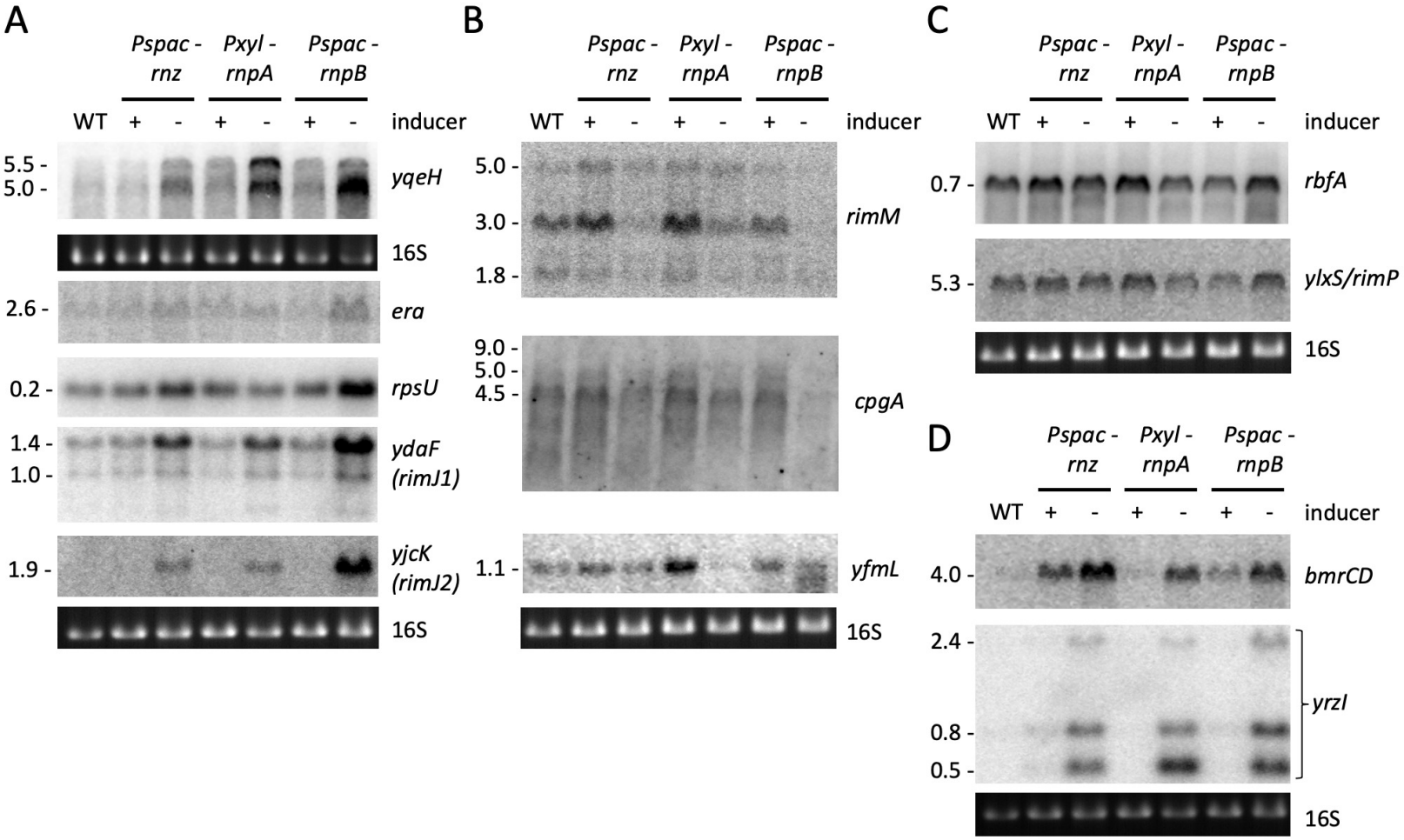
A
Pspac - rnz
Pxyl - rnpA
Pspac - rnpB
WT + - + - + - inducer
5.5 -
5.0 -
yqeH
16S
2.6 -
era
0.2 -
rpsU
1.4 -
1.0 -
ydaF (rimJ1)
1.9 -
yjcK (rimJ2)
16S
B
Pspac - rnz
Pxyl - rnpA
Pspac - rnpB
WT + - + - + - inducer
5.0 -
3.0 -
1.8 -
rimM
9.0 -
5.0 -
4.5 -
cpgA
1.1 -
yfmL
16S
C
Pspac - rnz
Pxyl - rnpA
Pspac - rnpB
WT + - + - + - inducer
0.7 -
rbfA
5.3 -
ylxS/rimP
16S
D
Pspac - rnz
Pxyl - rnpA
Pspac - rnpB
WT + - + - + - inducer
4.0 -
bmrCD
2.4 -
0.8 -
0.5 -
yrzI
16S

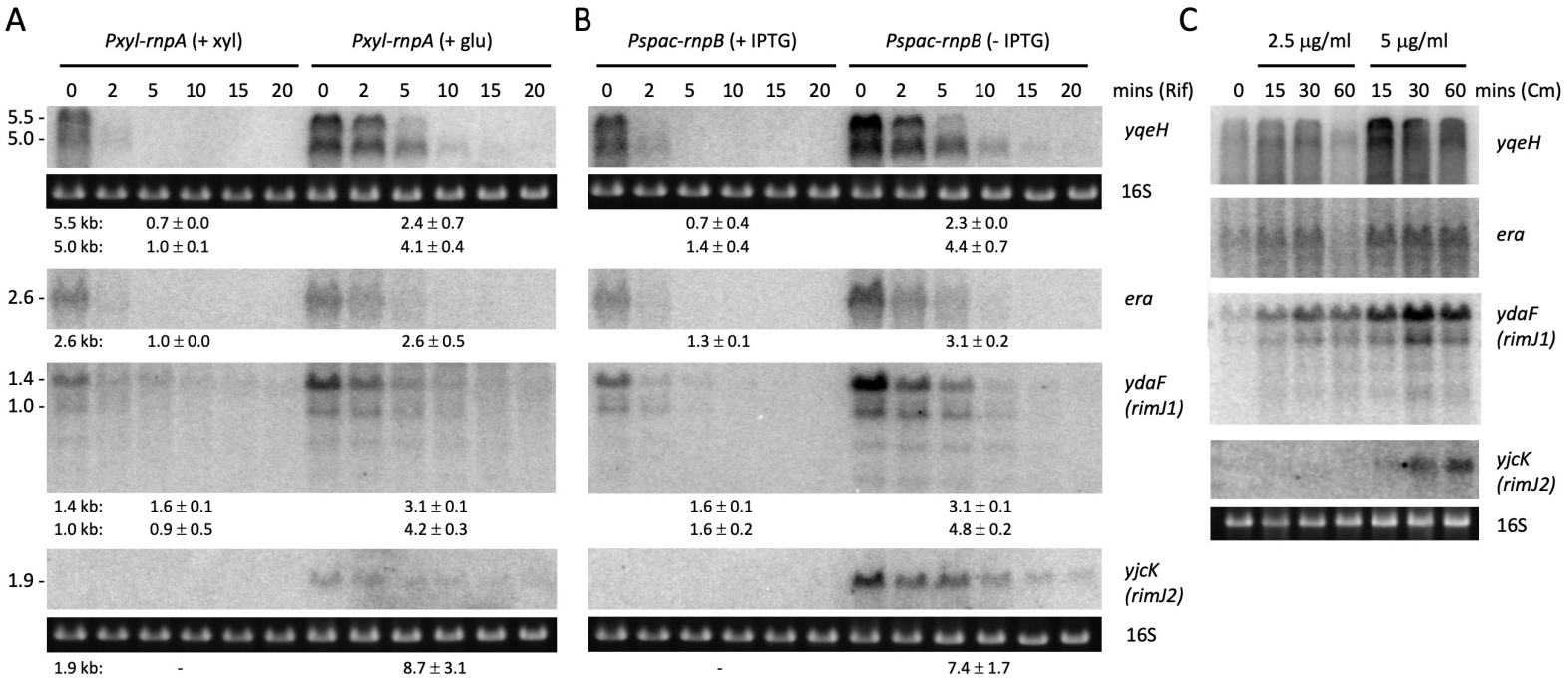
A
Pxyl-rnpA (+ xyl)
Pxyl-rnpA (+ glu)
0 2 5 10 15 20 0 2 5 10 15 20
5.5 -
5.0 -
5.5 kb: 0.7 ± 0.0 2.4 ± 0.7
5.0 kb: 1.0 ± 0.1 4.1 ± 0.4
2.6 -
2.6 kb: 1.0 ± 0.0 2.6 ± 0.5
1.4 -
1.0 -
1.4 kb: 1.6 ± 0.1 3.1 ± 0.1
1.0 kb: 0.9 ± 0.5 4.2 ± 0.3
1.9 -
1.9 kb: - 8.7 ± 3.1
B
Pspac-rnpB (+ IPTG)
Pspac-rnpB (- IPTG)
0 2 5 10 15 20 0 2 5 10 15 20
mins (Rif)
yqeH
16S
0.7 ± 0.4 2.3 ± 0.0
1.4 ± 0.4 4.4 ± 0.7
era
1.3 ± 0.1 3.1 ± 0.2
ydaF (rimJ1)
1.6 ± 0.1 3.1 ± 0.1
1.6 ± 0.2 4.8 ± 0.2
yjcK (rimJ2)
16S
- 7.4 ± 1.7
C
2.5 µg/ml
5 µg/ml
0 15 30 60 15 30 60 mins (Cm)
yqeH
era
ydaF (rimJ1)
yjcK (rimJ2)
16S

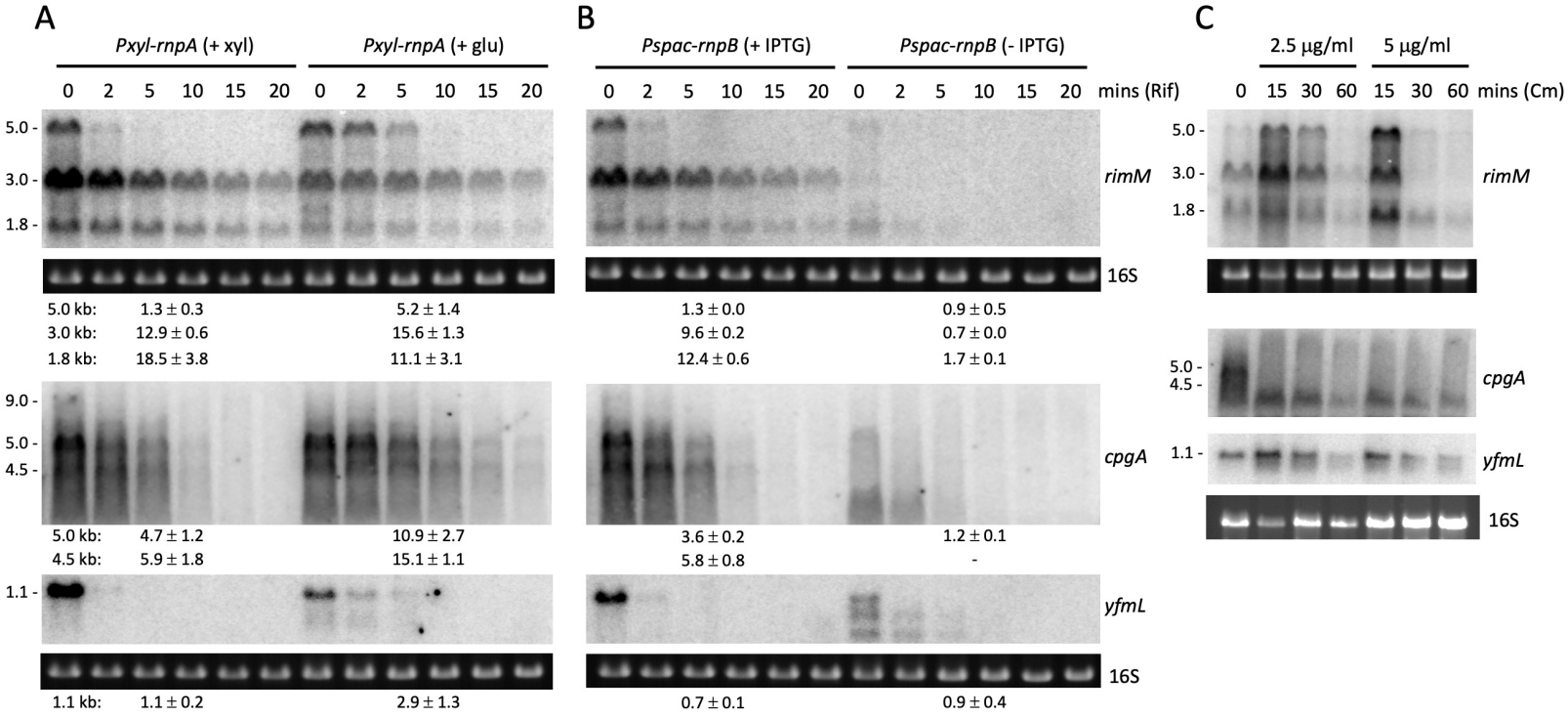
A
Pxyl-rnpA (+ xyl)
Pxyl-rnpA (+ glu)
0 2 5 10 15 20 0 2 5 10 15 20
5.0 -
3.0 -
1.8 -
5.0 kb: 1.3 ± 0.3 5.2 ± 1.4
3.0 kb: 12.9 ± 0.6 15.6 ± 1.3
1.8 kb: 18.5 ± 3.8 11.1 ± 3.1
9.0 -
5.0 -
4.5 -
5.0 kb: 4.7 ± 1.2 10.9 ± 2.7
4.5 kb: 5.9 ± 1.8 15.1 ± 1.1
1.1 -
1.1 kb: 1.1 ± 0.2 2.9 ± 1.3
B
Pspac-rnpB (+ IPTG)
Pspac-rnpB (- IPTG)
0 2 5 10 15 20 0 2 5 10 15 20 mins (Rif)
rimM
16S
1.3 ± 0.0 0.9 ± 0.5
9.6 ± 0.2 0.7 ± 0.0
12.4 ± 0.6 1.7 ± 0.1
cpgA
3.6 ± 0.2 1.2 ± 0.1
5.8 ± 0.8 -
yfmL
16S
0.7 ± 0.1 0.9 ± 0.4
C
2.5 µg/ml
5 µg/ml
0 15 30 60 15 30 60 mins (Cm)
5.0 -
3.0 -
1.8 -
rimM
5.0 -
4.5 -
cpgA
1.1 -
yfmL
16S

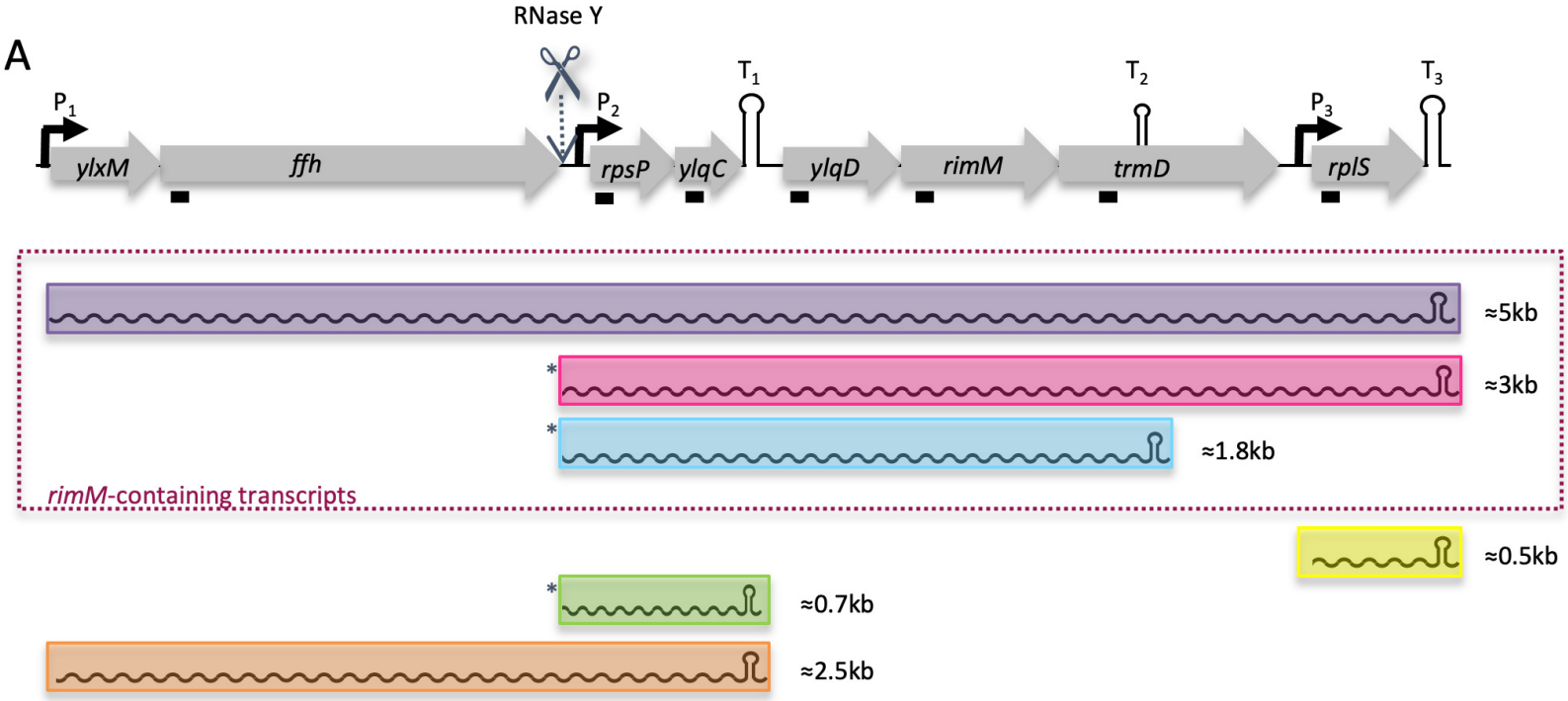
A
RNase Y
P1
P2
P3
T1
T2
T3
ylxM
ffh
rpsP
ylqC
ylqD
rimM
trmD
rplS
≈5kb
≈3kb
≈1.8kb
rimM-containing transcripts
≈0.5kb
≈0.7kb
≈2.5kb

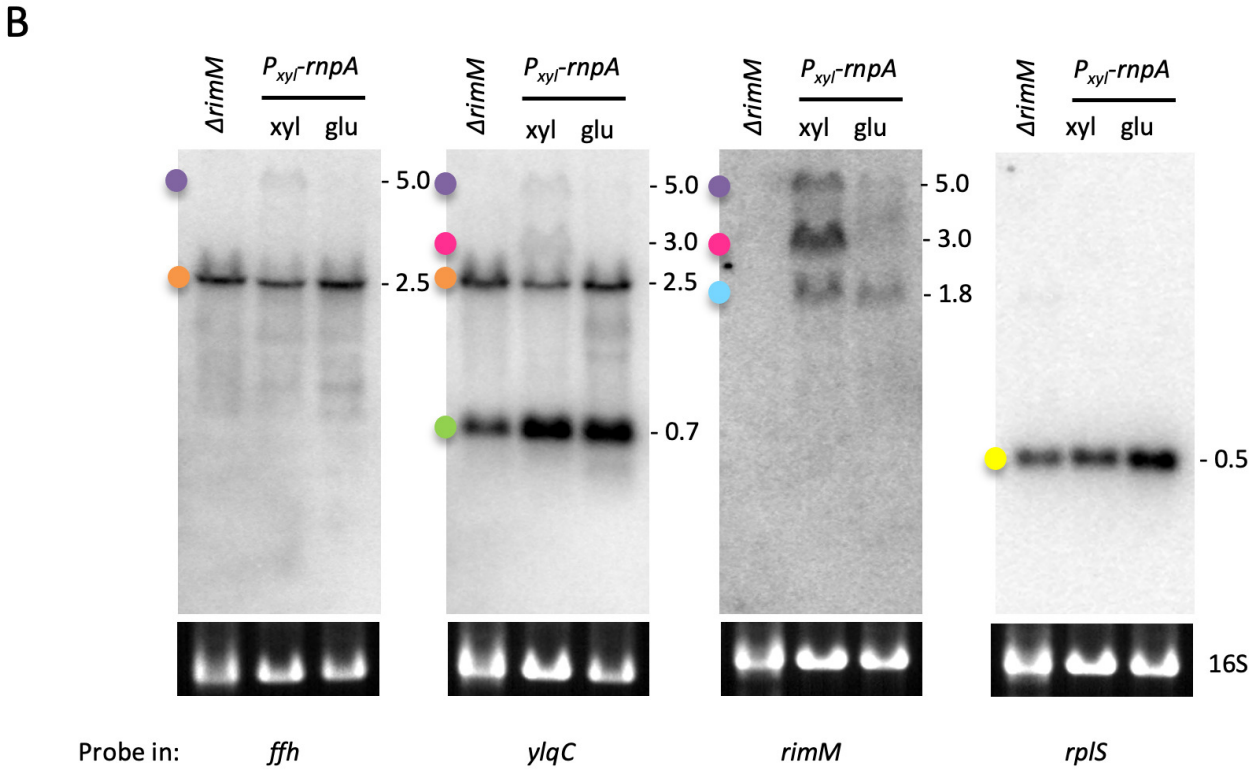
B
ΔrimM
Pxyl-rnpA
xyl
glu
- 5.0
- 2.5
- 3.0
- 0.7
- 1.8
- 0.5
16S
Probe in:
ffh
ylqC
rimM
rplS

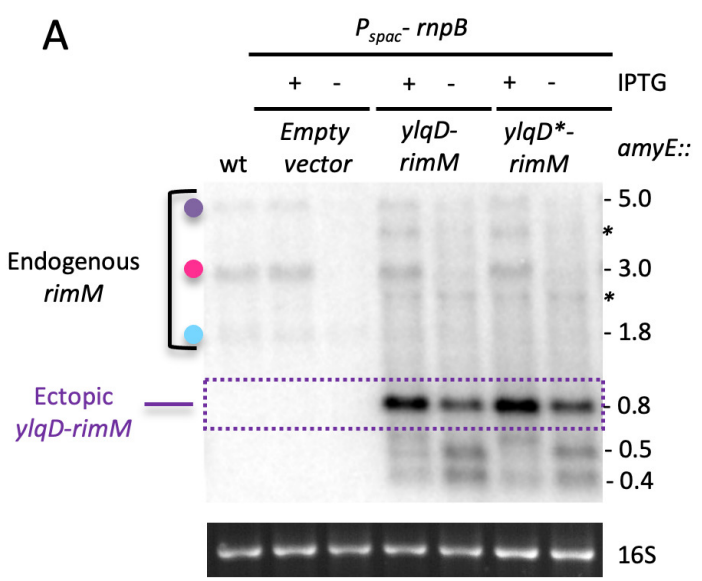
A
P_{spac}- rnpB
+ - + - + -
IPTG
wt
Empty vector
ylqD-rimM
ylqD*-rimM
amyE::
Endogenous rimM
Ectopic ylqD-rimM
- 5.0
*
- 3.0
*
- 1.8
- 0.8
- 0.5
- 0.4
16S

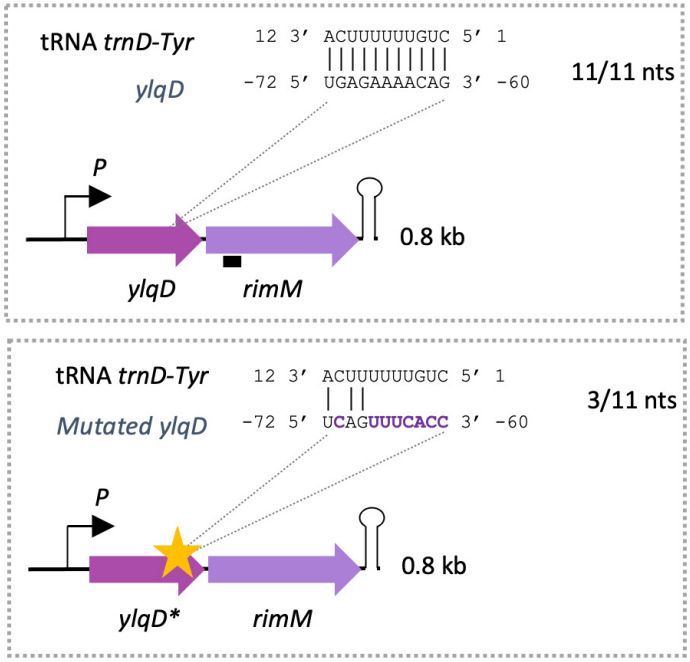
B
tRNA trnD-Tyr
12 3′ ACUUUUUUGUC 5′ 1
ylqD
-72 5′ UGAGAAAACAG 3′ -60
11/11 nts
P
0.8 kb
ylqD
rimM
tRNA trnD-Tyr
12 3′ ACUUUUUUGUC 5′ 1
Mutated ylqD
-72 5′ UCAGUUUCACC 3′ -60
3/11 nts
P
0.8 kb
ylqD*
rimM

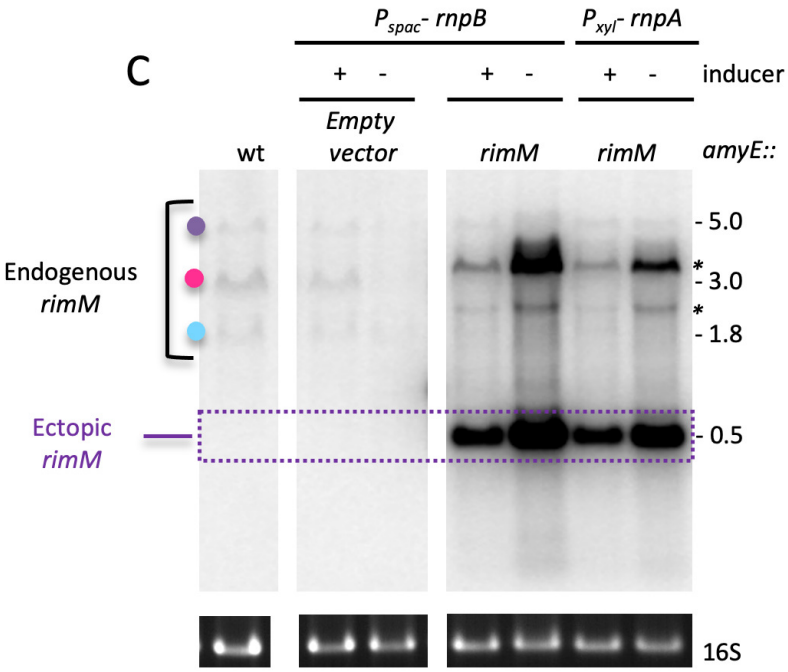
C
P_{spac}- rnpB
P_{xyl}- rnpA
+ - + - + -
inducer
wt
Empty vector
rimM
rimM
amyE::
Endogenous rimM
Ectopic rimM
- 5.0
*
- 3.0
*
- 1.8
- 0.5
16S

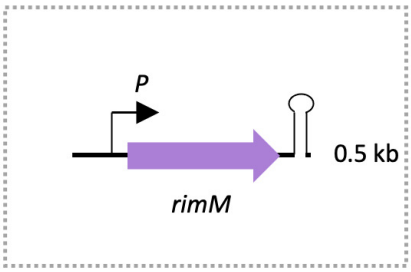
D
P
0.5 kb
rimM

A

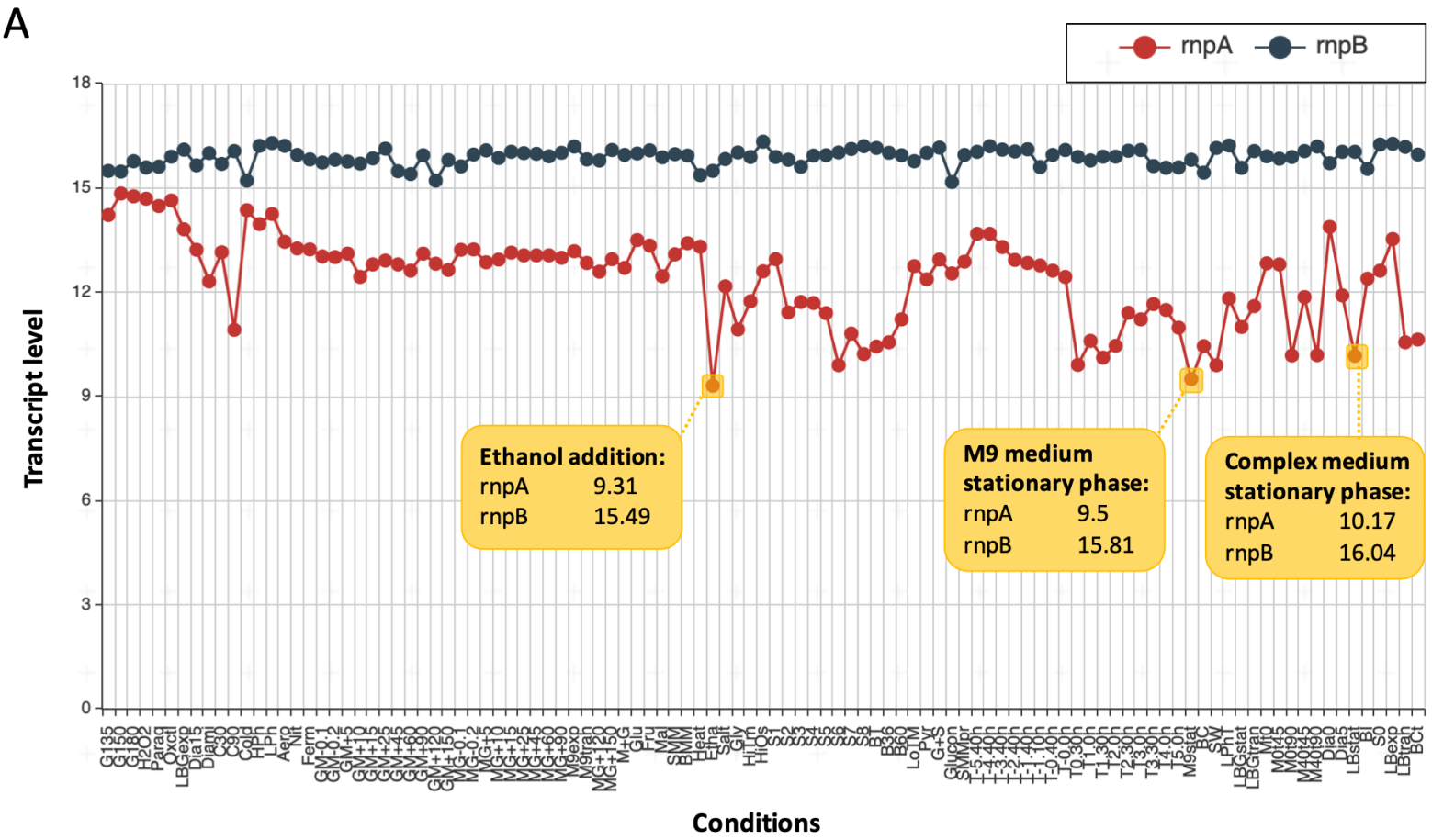
rnpA
rnpB
Transcript level
Conditions
Ethanol addition:
rnpA 9.31
rnpB 15.49
M9 medium stationary phase:
rnpA 9.5
rnpB 15.81
Complex medium stationary phase:
rnpA 10.17
rnpB 16.04

B

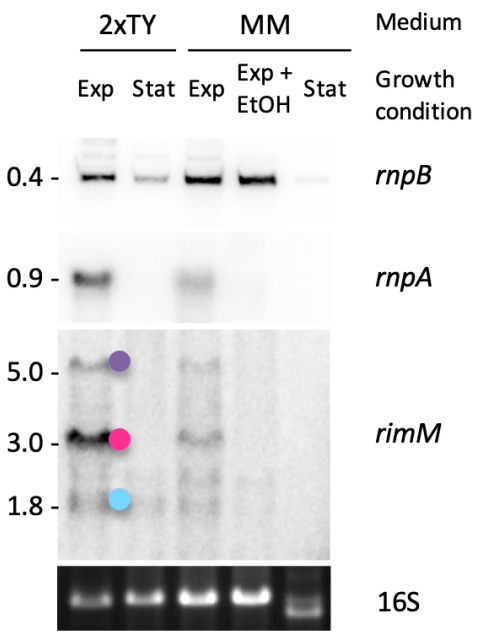
2xTY
MM
Medium
Exp
Stat
Exp
Exp + EtOH
Stat
Growth condition
0.4 -
rnpB
0.9 -
rnpA
5.0 -
3.0 -
1.8 -
rimM
16S

C

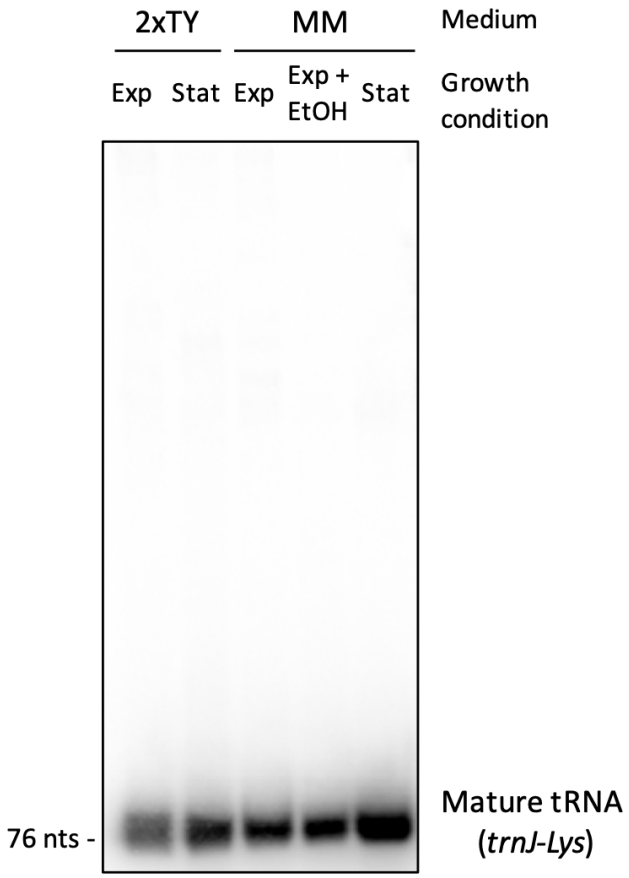
2xTY
MM
Medium
Exp
Stat
Exp
Exp + EtOH
Stat
Growth condition
76 nts -
Mature tRNA (trnJ-Lys)

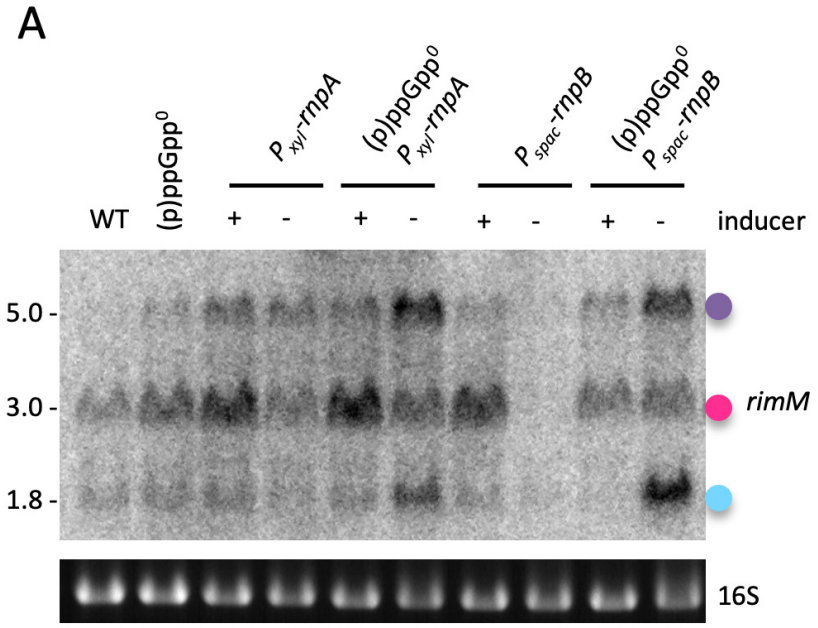
A
WT
(p)ppGpp0
Pxyl-rnpA
(p)ppGpp0 Pxyl-rnpA
Pspac-rnpB
(p)ppGpp0 Pspac-rnpB
+ - + - + - + -
inducer
5.0 -
3.0 -
1.8 -
rimM
16S

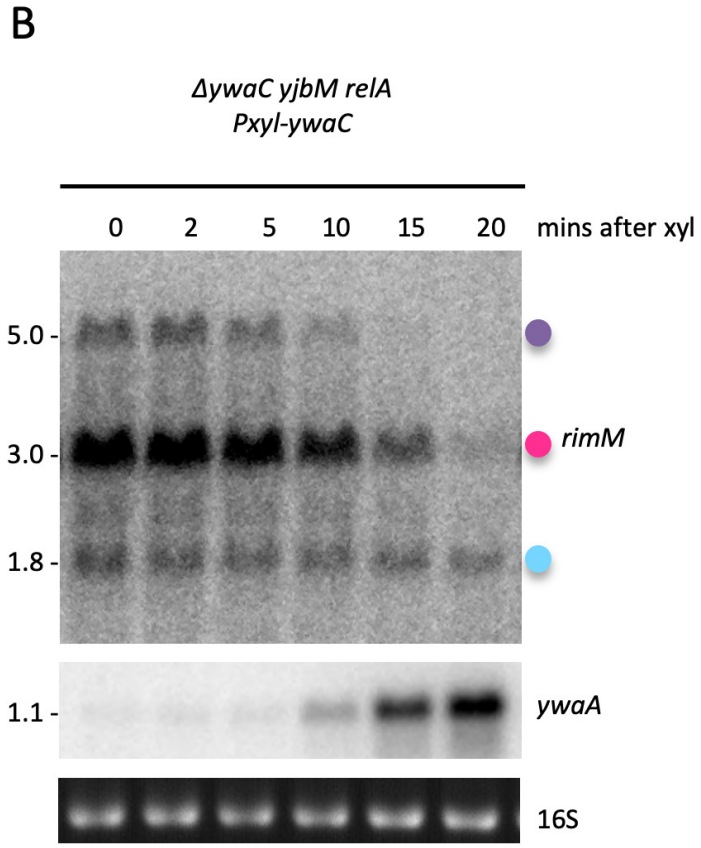
B
ΔywaC yjbM relA
Pxyl-ywaC
0 2 5 10 15 20
mins after xyl
5.0 -
3.0 -
1.8 -
rimM
1.1 -
ywaA
16S

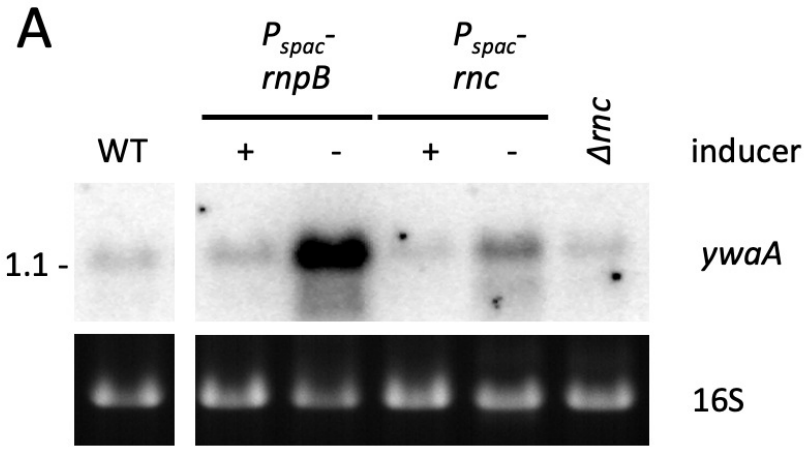
A
P_{spac}-
rnpB
P_{spac}-
rnc
WT
+
-
+
-
Δrnc
inducer
1.1 -
ywaA
16S

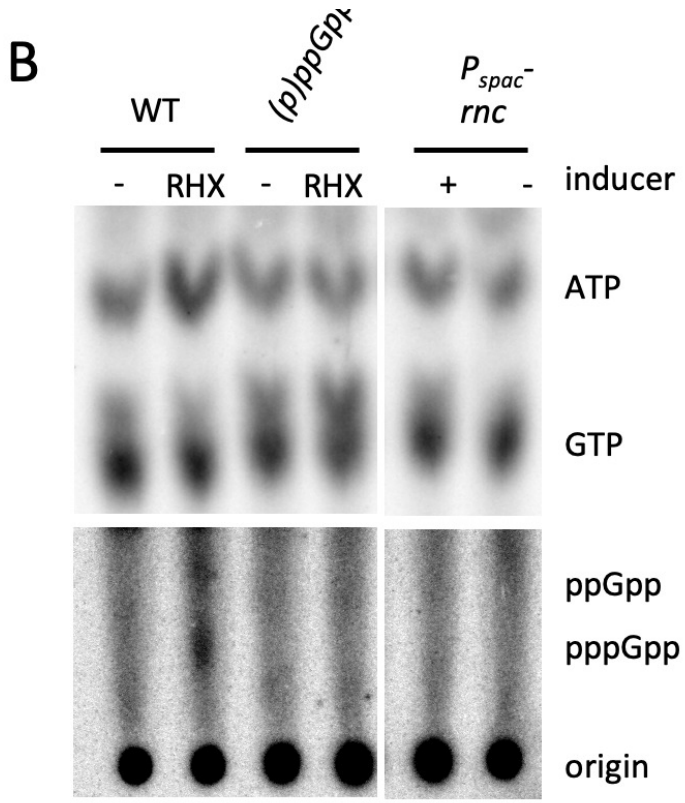
B
WT
(p)ppGpH
P_{spac}-
rnc
-
RHX
-
RHX
+
-
inducer
ATP
GTP
ppGpp
pppGpp
origin

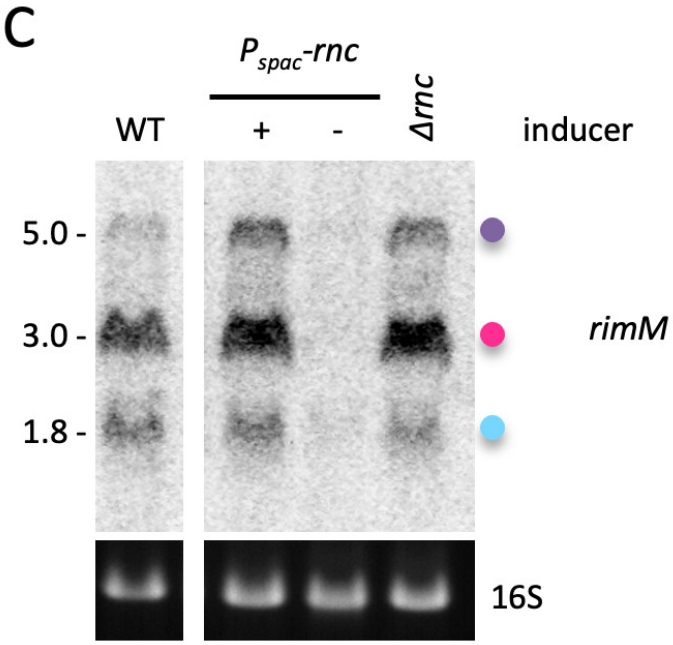
C
P_{spac}-rnc
WT
+
-
Δrnc
inducer
5.0 -
3.0 -
1.8 -
rimM
16S

Table S1: *B. subtilis* strains used in this study

Strains	Genotype	Reference
SSB318	W168 *Pspac-rnpB:pMUTIN ery*	(28)
SSB1002	W168 *trp+*	Lab strain
CCB288	W168 *amyE::Pspac-rnc Cm rnc::spc pMAP65*	(16)
CCB321	W168 *Pspac-rnz:pMUTIN ery* pMAP65 *kan*	(8)
CCB418	W168 *txpA -10Δ yonT::ery rnc::spc*	(16)
CCB504	W168 *Pxyl-rnpA Cm*	(8)
CCB664	W168 *rimM*::*ery*	(29); This study
CCB994	W168 *Pspac-rnpB:pMUTIN ery amyE::pHM2-ylqD-rimM Cm*	This study
CCB1008	W168 *Pspac-rnpB:pMUTIN ery amyE::pHM2-ylqD*-rimM Cm*	This study
CCB1014	W168 *Pspac-rnpB:pMUTIN ery amyE::pHM2 Cm*	This study
CCB1017	W168 *Pspac-rnpB:pMUTIN ery amyE::pHM2-rimM Cm*	This study
CCB1031	W168 *Pxyl-rnpA Cm amyE::pHM2-rimM Spc*	This study
CCB1050	W168 *yjbM::spc ywaC::kan relA::ery*	(8)
CCB1057	W168 *yjbM::spc ywaC::kan Pxyl-rnpA Cm relA::ery*	(8)
CCB1125	W168 *yjbM::spc ywaC::kan amyE::pX-ywaC Cm relA::ery*	(8)
CCB1137	W168 *yjbM::spc ywaC::kan Pspac-rnpB:pMUTIN relA::ery::tet*	(8)

Table S2. Details of strain construction

Strain number	Plasmid	Description	Source/Ref.
CCB994	752	Plasmid 752 linearized with XhoI and integrated into SSB318 *amyE* locus.	This study; (8)
CCB1008	762	Plasmid 762 linearized with XhoI and integrated into SSB318 *amyE* locus.	This study; (8)
CCB1014	606	Plasmid 606 linearized with XhoI and integrated into SSB318 *amyE* locus.	This study; (8)
CCB1017	764	Plasmid 764 linearized with SpeI and integrated into SSB318 *amyE* locus.	This study; (8)
CCB 1031	Plasmid 764 and pCS	First, plasmid 764 linearized with SpeI was integrated into *amyE* in WT. Then the plasmid 764 Cm cassette was switched to Spc using an antibiotic cassette switching vector (pCS). The resulting strain was then transformed with CCB504 gDNA.	This study; (8, 30)

Table S3: Plasmids constructed for this study

Plasmid number	Plasmid name	Initial vector	Insert	Oligos for PCR	Description	Source /Ref.
606	pHM2-Pspac(con)	pHM2	Pspac(con)		Promoter P_{spac} from pMUTIN-4M cloned without the operator sequence using EcoRI-HindIII restriction sites	This study; (31)
752	pHM2-Pspac(con)-ylqD-rimM	606	*ylqD-rimM*	CC1985 + CC1986	Insert amplified from gDNA and cloned in BamHI/SalI under plasmid 606 constitutive promoter.	This study
762	pHM2-Pspac(con)-ylqD*-rimM	606	*ylqD*-rimM*	CC1985 + CC2012; CC2011 + CC1986	ylqD* and *rimM* were amplified from plasmid 752. The CC2011/CC2012 oligos introduce mutations in *ylqD* ORF. *ylqD*-rimM* overlap was obtained by overlap PCR with underlined oligos and cloned in BamHI/SalI.	This study
764	pHM2-Pspac(con)-rimM	606	*rimM*	CC1986 + CC2034	Insert amplified from gDNA and cloned in BamHI/XhoI under plasmid 606 constitutive promoter.	This study

Table S4: Oligonucleotides used in this study

Oligo	Gene	Sequence
CC1005	*rnpA*	ACTGGCGGTTTGCAACTGATGTCCC
CC1006	*rnpB*	TGCGAGCATGGACTTTCCTCTACAG
CC1560	*rpsU*	CTAGCAGCTTCAGACTTTTTCTTGCGC
CC1841	*ylxS*	GAGTTCCAGCTGAAGGCTGTCTACGATTGGC
CC1842	*rbfA*	GCTTTTGCCAGCCCTTTCAGCGCTTCTTCCC
CC1845	*rimM*	GAAATCACCCGCACTTCGCCTTTGATTCCGTG
CC1846	*era*	CCTTGTTTCTCGTCGTTTGGGGCTTATCGC
CC1847	*yqeH*	CGACCAGAGAGTCCGTTTCTCCAATACCGTG
CC1915	trnJ-lys	GACTCGAACCTTCGACCCTCTGATTAAAAG
CC1985	ylqD fw	TAAGGATCCGCTTAGGCAAAATAGAAAAGCCTGGACGAG
CC1986	rimM rvs	TAACTCGAGAAAAAGGCCATCCGTCAGGATGGCCGAGCACGCCTTCAAACATTTa GGGAAACAGCG
CC2011	ylqD* fw	GGGGATGACTGGCATcAGtttcaccCAGCGAACACCATCGTC
CC2012	ylqD* rvs	GACGATGGTGTTCGCTGggtgaaaCTgATGCCAGTCATCCCC
CC2034	rimM fw	ATATGGATCCTGGAAGAGGTGATCATATGACAAAGCGATGG
CC2099	*ylqD*	CTCGGTTAAGACTTGCATAACGGCTACACGG
CC2100	*ylqC*	GTCATCTGGATGATCAACAAGCGGCGTCAC
CC2101	*trmD*	CTGCCTTTGATGTCAGGTCCTCGACCGCGTC
CC2103	*ffh*	GAAATCGTCTGCTGCAGTCGGTCGGCTAATC
CC2143	*rpsP*	GATGAAACGGCCGTCACGTGGTGAACGAGAATC
CC2144	*rplS*	CAGGACGGAACGCAGGAAGATCAGTACGAAG
CC2197	*yjcK*	CGAAACCGTCCCGATTAATCTATCGTCTGACG
CC2198	*ydaF*	GATTGTTTCTCGGTACGTGTCAGCGCTGCTTG
CC2199	*yfmL*	GACGAGCTGATCCGTTTCATCAAGCACGATC
CC2200	*cpgA fwd*	CAACGAGCTTATCAGGCCGCCAATTTGCAAC
CC2201	*cpgA + PT7 rvs*	gctctaatacgactcactatagggACGTGTGAATCAGCTCCACGTGGCGGG
CC2213	*ywaA*	GATGCAGAGGCGGTCGTTTGATTGATTCAG
CC2215	*ilvA*	CACATCCGGATCATCGAACGGATGGATAAACGTC
CC2450	*ksgA*	CTGTTTTCTCCGTCACTTCCGCGTGATCAAC

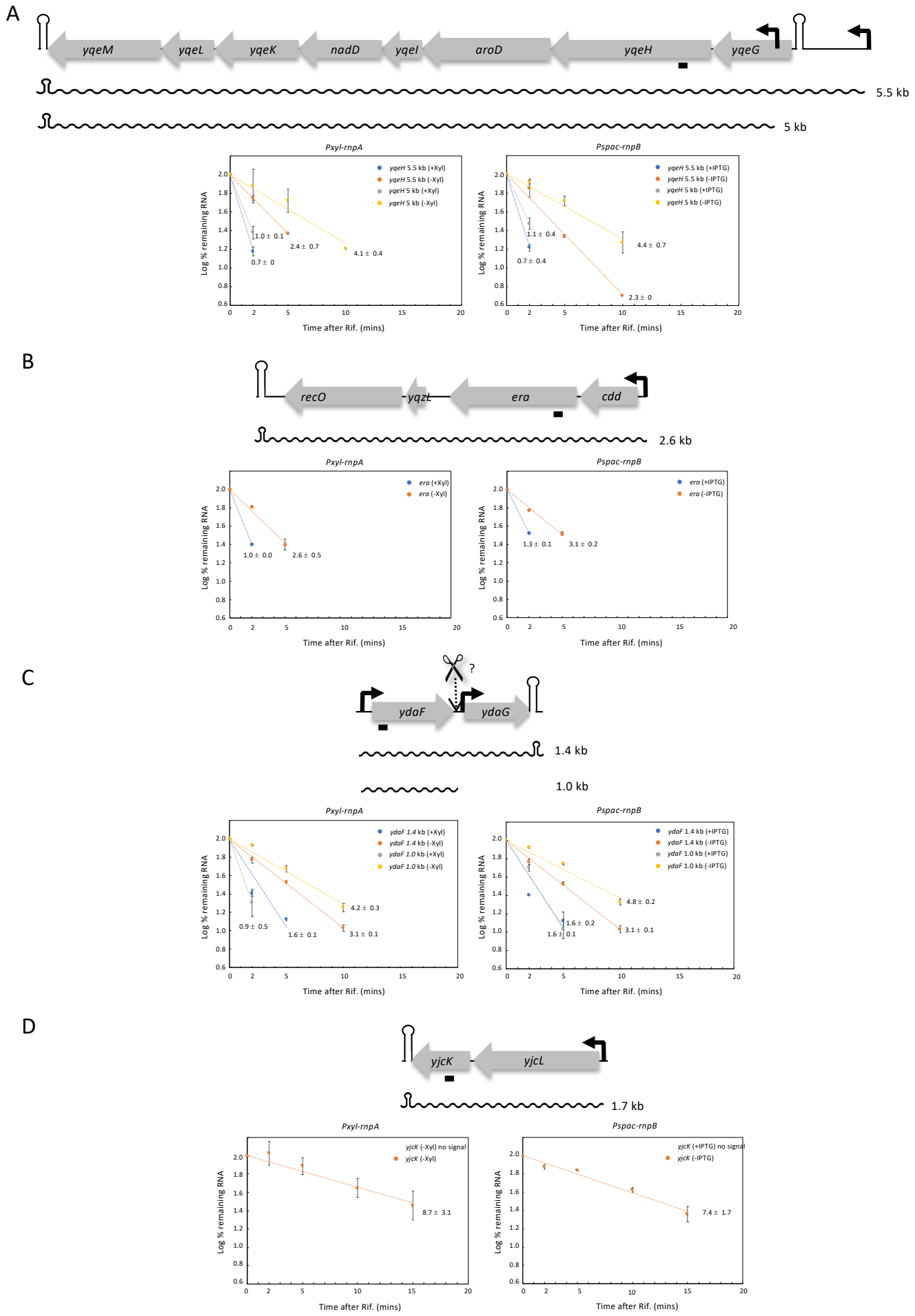

Figure S1: Schematics and RNA decay plots of up-regulated transcripts in RnpA and RnpB-depletion strains. Open reading frames (ORFs; not to scale) are shown as gray arrows and transcripts as wavy lines. Sizes are as indicated. Promoters are represented by black arrows and terminators as hairpins. Suspected endoribonucleolytic cleavage sites are indicated by a scissors symbol with a question mark. Quantifications are from the average of two experiments, with half-lives as indicated.

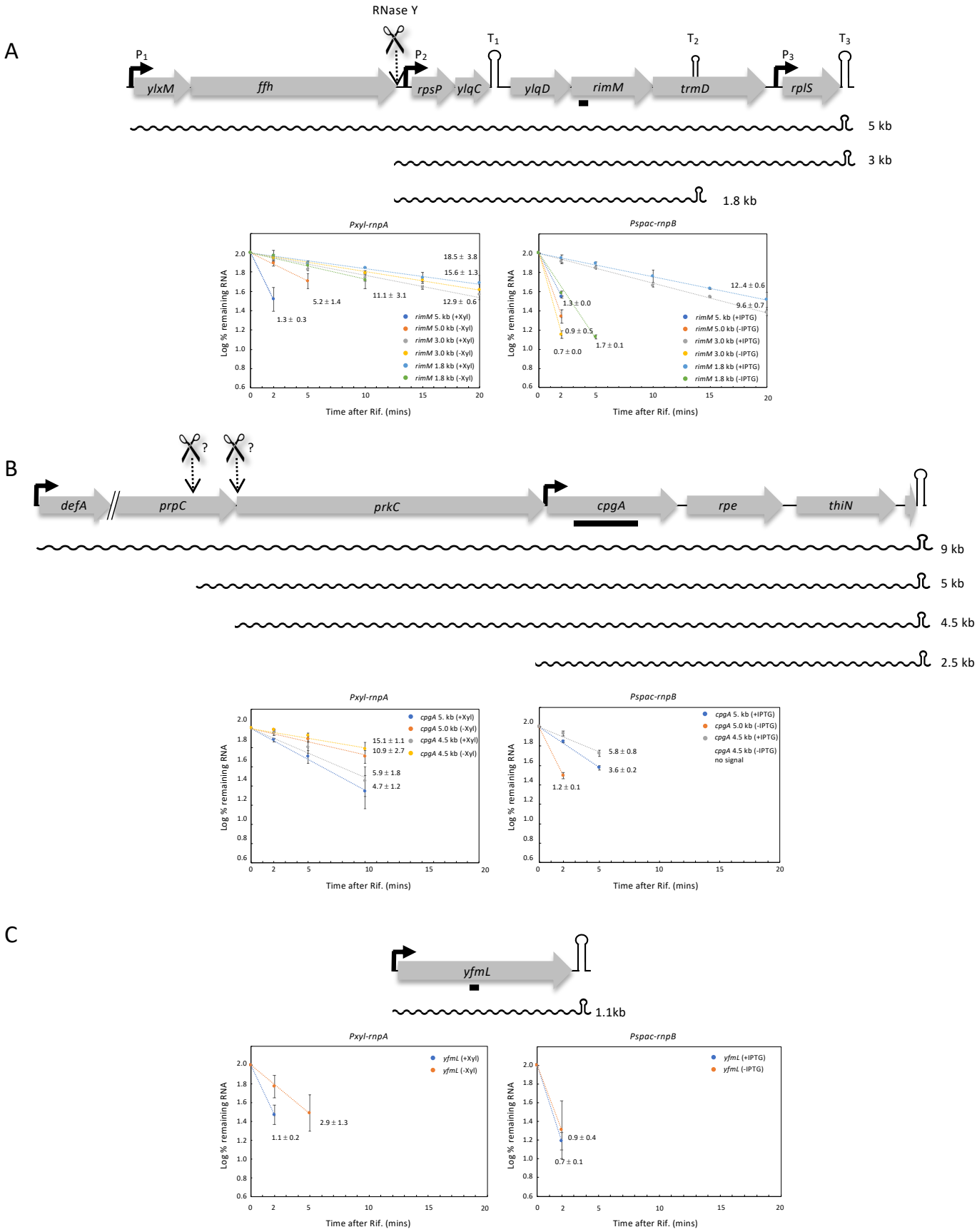

Figure S2: Schematics and RNA decay plots of down-regulated transcripts in RnpA and RnpB-depletion strains. Open reading frames (ORFs; not to scale) are shown as gray arrows and transcripts as wavy lines. Sizes are as indicated. Promoters are represented by black arrows and terminators as hairpins. Suspected endoribonucleolytic cleavage sites are indicated by a scissors symbols with question marks. Quantifications are from the average of two experiments, with half-lives as indicated.

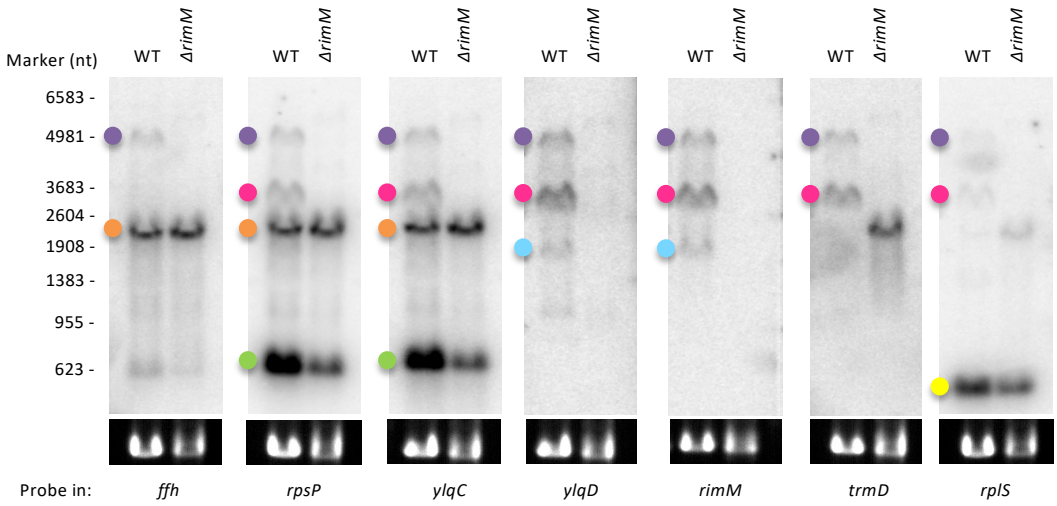

Figure S3: Northern blot analysis to determine the structure of the *rimM* operon. Total RNA from WT or *ΔrimM* strains was probed with oligonucleotides targeting different ORFs of the *rimM* operon (indicated below each panel). 16S rRNA levels (ethidium bromide stained) are shown as a loading control. The *ffh* and *ylqC* blots were stripped and reprobed for *rplS* and *ylqD*, respectively. Colored dots correspond to the color of transcripts shown in Figure 4A.

	levels			stability		Cm		ppGpp°		ppGpp⁺	growth rate
	rnz	*rnpA*	*rnpB*	*rnpA*	*rnpB*	sub	MIC	*rnpA*	*rnpB*	-	*rnc*
FL	-	-	↓	↑	-	↷	↷	↑	↑	↓	↓
Y/P_2-T_3	↓	↓	↓	-	↓	↷	↷	-	↑	↓	↓
Y/P_2-T_2	↓	↓	-	-	↓	↷	↷	↑	↑	-	↓

Figure S4. Summary of effects on 3 three *rimM* containing transcripts. Data are taken from Northern blots shown in Figures 1 (levels), 2-3 (stability, Cm), 6A (ppGpp^0), 6B (ppGpp$^+$) and 7 (growth rate). Depleted tRNA maturases are indicated. Transcripts are listed according to size: full-length (FL), RNase Y/P_2-T_3 and RNase Y/P_2-T_2. Red arrows show down-effects, green arrows show up-effects, (-) no effect. Curved arrow in sub-inhibitory Cm condition (sub) reflects initial increase followed by decrease.

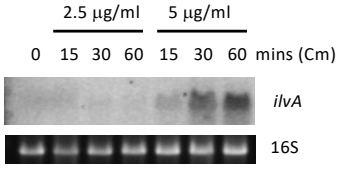

Figure S5. Induction of expression of the CodY regulon member *ilvA* by chloramphenicol. Northern blots of total RNA isolated at different times after addition of 0.5x MIC and MIC of chloramphenicol (Cm). 16S rRNA levels (ethidium bromide stained) are shown as a loading control.